NACA RM E50I14

RESEARCH MEMORANDUM

EXPERIMENTAL INVESTIGATION OF AIR-COOLED TURBINE BLADES IN TURBOJET ENGINE

II - ROTOR BLADES WITH 15 FINS IN COOLING-AIR PASSAGES

By Robert O. Hickel and Herman H. Fleischbrock, Jr.

Lewis Flight Propulsion Laboratory
Cleveland, Ohio

NATIONAL ADVISORY COMMITTEE FOR AERONAUTICS

WASHINGTON

NATIONAL ADVISORY COMMITTEE FOR AERONAUTICS

RESEARCH MEMORANDUM

EXPERIMENTAL INVESTIGATION OF AIR-COOLED TURBINE BLADES IN TURBOJET ENGINE

II - ROTOR BLADES WITH 15 FINS IN COOLING-AIR PASSAGES

By Robert O. Hickel and Herman H. Ellerbrock, Jr.

SUMMARY

An investigation is being conducted to determine experimentally the effectiveness of air-cooling several configurations of turbine blades in a turbojet engine. The results obtained with the second blade configuration, a hollow blade shell with 15 fins inserted, are presented.

The turbine of a commercial turbojet engine was modified for this investigation by replacing two of the original blades that were diametrically opposite one another with hollow air-cooled blades that had 15 fins inserted in the hollow blade shell. The air-cooled blades were instrumented so that the radial temperature distribution near the trailing edge and the peripheral temperature distribution approximately one-third of the spanwise distance from the blade base could be determined. Investigation of the cooled-blade temperature distribution was made over a range of cooling-air flows from 0.005 to about 0.125 pound per second per blade. The engine speed was varied from 4000 to 10,000 rpm and the combustion-gas-flow rate from 20.4 to 62.9 pounds per second.

Comparisons of the cooling obtained with the 15-fin blade were made with the cooling of a 10-tube blade investigated earlier. The results showed that the 15-fin blade cooled appreciably better than the 10-tube blade at a point near the midchord. For example, at an engine speed of 10,000 rpm, a cooling-air temperature at the blade root of 70° F, a ratio of coolant flow to combustion-gas flow of 0.05, and an effective gas temperature (or solid-blade temperature) of 980° F, the temperature on the convex side of the 15-fin blade was about 104° F lower than that of the 10-tube blade (357° F compared with 461° F), whereas the temperature on the concave side of the 15-fin blade was about 70° F lower. For points near the leading and trailing edges of

the blades, the temperatures at the given operating conditions were quite similar for the 15-fin and 10-tube blades. The temperatures near the leading and trailing edges of the 15-fin blade were about 13° F hotter (802° F compared with 789° F) and 48° F cooler (767° F compared with 815° F), respectively, than those of the 10-tube blade.

Calculations of the allowable turbine-inlet temperatures for the 15-fin blade, based on the simple centrifugal stresses at design speed and a coolant- to combustion-gas-flow ratio of 0.05, are presented. It was indicated that for a nonstrategic metal the allowable turbine-inlet temperature based on the trailing-edge temperatures would be about 1380° F, whereas if the entire blade could be cooled to the temperature at the midchord the calculated allowable turbine-inlet temperature would be approximately 2370° F.

INTRODUCTION

An investigation of air-cooled turbine blades of various configurations installed in the turbine of a commercial turbojet engine was conducted at the NACA Lewis laboratory in order to: (1) obtain cooled turbine-blade configurations of nonstrategic blade materials that will permit operation of the engine at current turbine-inlet temperatures and (2) achieve improved engine performance by extending the application of cooled turbines to higher gas temperatures while still using nonstrategic materials if at all possible.

The initial fundamental research on cooled blades in cascades and in individual turbines and the development of the theory that formed the basis for this present investigation are discussed in reference 1. The basic design considerations, blade modifications, engine alterations, method of blade fabrication, and so forth that are common to this investigation are also discussed in reference 1.

The first air-cooled blades of the investigation were untwisted and slightly tapered from root to tip. The root profile was the same as that at the root of the conventional uncooled blades installed in the turbine of the commercial engine used in the investigation. In order to increase the internal heat-transfer surface area, 10 tubes were inserted in the hollow shells of these air-cooled blades. The results with these blades (reference 1) indicated that the blade cooling was excellent except for the leading and trailing edges. Calculations showed, however, that the temperature of the leading and trailing edges would have to be decreased before current turbine-inlet temperatures could be utilized with nonstrategic blade materials and a cooling-air flow equivalent to 5 percent or less of the combustion-gas flow.

Another method of increasing the surface in contact with the cooling air inside the blade shell is to place fins (strips of metal) inside the shell. The edges of the fins are embedded in the blade shell. In order to compare the blade cooling obtained with the 10 tubes (reference 1) with that of a finned blade, the second blade configuration selected for investigation was one having 15 fins inserted in the blade shell. The cooling results of this second configuration are reported herein. The engine modifications and instrumentation were essentially the same type as those of reference 1. The cooled-blade temperatures were obtained over a range of cooling-air flows at several constant engine speeds from 4000 to 10,000 rpm. The cooling-air flow per blade was varied from a minimum required for safe operation of approximately 0.005 pound per second to about 0.125 pound per second. This variation corresponds to a range of the ratio of cooling-air flow to combustion-gas flow of about $1\frac{1}{4}$ to 32 percent at 4000 rpm and about 1/2 to 11 percent at 10,000 rpm.

SYMBOLS

The following symbols are used in this report:

g	acceleration due to gravity, (ft/sec^2)
N	engine speed, (rpm)
n	exponent
P	pumping power from hub to blade tip, (hp)
p	static pressure, (in. Hg absolute)
p'	total pressure, (in. Hg absolute)
R	ratio of cooling-air flow per blade to combustion-gas flow per blade
r	radius from center of rotor, (ft)
T	static temperature, ($^{\circ}R$ or $^{\circ}F$)
T'	total temperature, ($^{\circ}R$ or $^{\circ}F$)
V	absolute velocity, (ft/sec)

w weight-flow rate, (lb/sec)

$\Delta p'$ pressure rise

η efficiency of compression in turbine wheel

Λ temperature recovery coefficient of modified solid blade

ρ density, (slugs/cu ft)

φ temperature-difference ratio, $\left(T_{g,e} - T_B\right) \Big/ \left(T_{g,e} - T_{a,e,h}\right)$

ω angular velocity of rotor, (radians/sec)

Subscripts:

A combustion air

a blade-cooling air

B cooled blade

c compressor

e effective

f fuel

g combustion gas

H hub of rotor

h root of blade

i inlet

m mixture of combustion gas and scavenge, bearing, and blade-cooling air in tail pipe

o outlet

S stator

T blade tip

u tangential component

0 NACA sea-level air

APPARATUS

A commercial turbojet engine (of the same type as used in reference 1) was modified and instrumented so that the cooled-turbine-blade temperature could be experimentally compared with the uncooled-blade temperatures during engine operation. The engine employed had a dual-entry centrifugal compressor and a combustion-chamber assembly consisting of 14 individual burners and a single-stage turbine.

General Engine Modifications

Blading modifications. - Two of the original 54 turbine blades were replaced by untwisted hollow blades with fins inserted. One of these blades is shown in figure 1. The cooled blades were placed in the turbine rotor at diametrically opposite positions. In addition, two of the original blades of the engine on the concave side and one on the convex side of each of the air-cooled blades were removed and replaced by solid untwisted blades of the same outside geometry as the cooled blades. This change was made to minimize unfavorable flow conditions around the untwisted cooled blades, as explained in reference 1. A typical arrangement of modified cooled and uncooled blades in the turbine rotor is shown in figure 2.

Cooling-air-supply arrangements. - Cooling air was supplied to the blades from an external source through an arrangement that was essentially the same as that described in reference 1. In brief, cooling air was fed into a modified tail cone to a duct that was concentric with and on the center line of the turbine rotor. The air passed through this duct, through a housing, and then through two radial tubes welded to the face of the rotor. The end of each radial tube near the rim of the turbine disk was fitted into a hole in the disk. The air passed through each hole in the disk to the bottom of serrated grooves that held the blade. At the bottom of each serrated groove, a slot was machined to extend to the drilled hole and thus provide a relatively smooth passage to the blades.

Scavenge air for the tail cone and cooling air for the bearing used in the blade cooling-air arrangement were also supplied in the same manner as described in reference 1.

Detailed Description of Modified Blading

General construction. - As in the case of the first configuration investigated (reference 1), the two cooled and six uncooled untwisted blade sections were cast and then welded to serrated bases cut from the conventional turbine blades. These bases were modified to provide entry for the cooling air to the root of the blade (See fig. 1.). This method was used in preference to casting the blade and the base as an integral unit because of the additional casting difficulties with the integral method, especially in the case of the hollow blades. The additional time required to machine the serrated grooves in the blade base was another deciding factor.

Blade fabrication. - The hollow and the solid modified blade sections were of cast high-temperature alloy X-40 and the serrated base material, as obtained from the conventional blade, was cast AMS-5385. The profiles of these blades were the same as those of the blades discussed in reference 1. The root section was the same as the profile at the root of the conventional blades used in the turbine. The hollow blades were so cast that the core area was constant over the length of the blade and the outside wall tapered linearly from the base to the tip. The nominal thickness of the wall at the base was 0.070 inch and at the tip, 0.040 inch. The modified solid blade tapered in like manner from root to tip. An end (top) view of the cooled-blade profile at the tip is shown in figure 1(a).

In order to increase the heat-transfer surface in contact with the cooling air, fifteen 0.020-inch thick fins made of SAE 1015 steel were inserted in slots cut spanwise in the walls of the hollow blade shells. The fins extended from a point about 7/16 inch above the blade root to a point about 5/32 inch from the blade tip. The fins were spaced about 5/64 inch apart starting at a point about 1/4 inch (measured along the chord line) from the leading edge of the blade. The fins were furnace-brazed in place with a commercial brazing material, and the outside blade surface was then ground to produce a smooth surface.

The conventional blade bases were modified by removing a portion of the blade base as shown in figures 1(b) and 1(c). An air-inlet slot was then burned through the base with an electrode. The profile of the air-inlet slot corresponded to that of the core of the blade.

Instrumentation

Engine instrumentation. - The same type engine instrumentation described in reference 1 was used in the investigation of the 15-fin blades. In addition, total- and static-pressure measurements were obtained immediately upstream of the rotor in the blade cooling-air-supply duct, as shown in figure 3. These pressure measurements were used in ascertaining the upstream pressure required to force the air through the system. In addition, the measured coolant-inlet pressure provided a means for evaluating pressure loss for this and subsequent cooled-blade configurations.

Blade instrumentation. - The temperature data presented herein are for thermocouple positions located as shown in figure 4. As shown in this figure, temperatures were obtained at three locations on one cooled blade, at four locations on the other, and at the leading edge and trailing edge of one modified uncooled blade (that is, the blade next to the cooled blade with trailing-edge thermocouples A, C, and D). Cooling-air temperatures were also obtained at the root of each cooled blade at locations E and K.

Coolant-flow measurements. - The coolant-flow measurements were made in the same manner as those described in reference 1.

TEST PROCEDURE

Cooling-tests procedure. - A number of series of runs with varying test conditions were made during this investigation. For each series, the engine speed was held constant and the blade-cooling air was varied by manually operated valves located in the supply line. Also for each series, a certain grouping of not more than six thermocouples could be connected at one time because of the limitation of the pickup system, as described in reference 1.

Method of investigation. - The first investigation made was to compare the temperatures on the cooled blades at approximately the same locations and to compare the temperatures of the cooling air just before it entered the blade roots. The grouping of the thermocouples for this series was C and I (trailing-edge thermocouples at 35-percent span) and E and K (cooling-air temperature at blade root). Temperature readings obtained on the potentiometer for thermocouples C and I and E and K were compared to determine the uniformity of cooling-air-flow conditions to the two diametrically opposite blades. These runs were made at an engine speed of 4000 rpm.

In order to determine the effect of the variation of the cooling-air flow on blade and cooling-air temperatures, investigations were then conducted first with thermocouple grouping A, C, D, E, and L (to determine the spanwise temperature distribution) and then with grouping G, H, I, J, K, and F (to determine peripheral temperature distribution) for two speeds, 4000 and 4900 rpm. During these investigations, it was found that the temperature of thermocouple L (trailing-edge temperature on solid blade) was considerably affected by the coolant flow from the adjacent cooled blade. Because of this influence from the cooled blade, thermocouple L could not be used as a reliable value for the effective gas temperature and consequently it was abandoned for the runs at higher speeds, and thermocouple F (leading edge of solid blade) was used exclusively for values of effective gas temperature. The cooled-blade thermocouple groupings for engine speeds of 5400 rpm and above were A, C, and D (spanwise thermocouples) and G, H, I, and J (peripheral thermocouples). Thermocouples E and F were also used with the first grouping and K and F, with the second grouping.

Before each series above 6000 rpm, a few points with different cooling-air flow were taken at either 4000 or 6000 rpm to check with previously obtained data. In this manner discrepancies in data and malfunctioning of instrumentation were detected. A visual check for cracks or defects in the cooled blades was made after speeds of 8000, 9000, and 10,000 rpm.

Test conditions. - The summary of conditions under which the investigation on the 15-fin blades was conducted is given in table I for each series of runs made. For the various series, the nominal engine speed varied from 4000 to 10,000 rpm, the engine gas flow from 20.4 to 62.9 pounds per second, and the turbine-inlet total temperature from 880° to 1167° F. The cooling-air flow per cooled blade varied from 0.005 to 0.129 pound per second and the temperature of the cooling air at the roots of the cooled blades varied from 44° to 135° F.

CALCULATION PROCEDURES

Correlation of cooled-blade temperatures. - From the equation for determining the spanwise temperature of air-cooled turbine blades given in reference 2, it was shown in reference 1 that the following equation is applicable:

$$\varphi \approx f(w_a, w_g) \tag{1}$$

where

$$\varphi = \frac{T_{g,e} - T_B}{T_{g,e} - T_{a,e,h}} \tag{2}$$

As a first approximation, the temperature-difference ratio φ can be plotted against the cooling-air flow for each engine speed and for each thermocouple position on the cooled blades. Such curves should be approximately applicable to all cooling-air and gas temperature conditions.

The data on the 10-tube blade of reference 1 were plotted in this manner with good correlation for most thermocouples. This method is therefore used herein to correlate the 15-fin-blade temperature data.

In order to correlate the data, the effective gas temperature $T_{g,e}$, which is the modified uncooled-blade temperature, is needed as shown in equation (2). At 4000 and 4900 rpm (series 2 and 4 in table I), no uncooled-blade temperature was obtained that could be used for $T_{g,e}$ to correlate the cooled-blade-temperature data. In order to obtain such a temperature for these runs, a curve of measured tail-pipe temperature against the leading-edge temperature of the solid blade (thermocouple F) for series 3 and 5 to 15 was first plotted. The curve is shown in figure 5. This curve and the measured tail-pipe temperatures for series 2 and 4 were then used to obtain the solid-blade temperatures, or $T_{g,e}$, for these series.

Correlation of solid-blade temperatures. - In order to calculate the cooled-blade temperatures from curves established from data of φ against w_a for several engine speeds for any engine and atmospheric conditions, it is necessary that $T_{g,e}$ be calculable for these conditions. It is shown in reference 1 how the solid-blade temperatures, or $T_{g,e}$, can be correlated through use of a recovery factor Λ; or in reverse manner, how Λ can be used to calculate the solid-blade temperatures. A method is fully described in reference 1 for using a recovery-factor curve obtained on a cascade of blades for calculating $T_{g,e}$ or the solid-blade temperatures. In the first investigation, a comparison was made between the calculated temperatures and the measured temperatures. The agreement was very good. As a consequence, the same method has been used in the present investigation to calculate the modified uncooled-blade temperatures for the conditions of the runs and the calculated and the measured temperatures (thermocouple F) are compared.

Correlation of pressures required for cooling. - The change in cooling-air pressure from the hub of the turbine rotor to the station where the pressure rake used for measuring the combustion-gas flow was located in the tail cone downstream of the rotor blades includes momentum changes, friction and expansion losses in the cooling passages, expansion losses from the blade tips, and a pressure change due to rotation of the turbine rotor that acts as a compressor. A method of comparing the cooling-air pressure drop through one blade configuration with that of another would be to plot the product of the inlet density of the cooling air and the difference between the inlet pressure in the supply tube and the pressure in the tail cone against the cooling-air flow for each engine speed for each blade. At a given cooling-air flow and engine speed, the blade that required the highest value of density times pressure difference would be the most costly for cooling. This method would require curves for each speed and one that would give a comparison, although use of only one curve for each blade would be much more convenient.

From the Euler equation,

$$P = \frac{w_a \omega}{550\ g}\left(r_T\ V_{u,a,T} - r_H\ V_{u,a,H}\right)$$

it can be shown on the basis of references 3 and 4 that the pressure rise of the cooling air through the turbine rotor from hub to tip can be approximately represented by the equation

$$\Delta p'_{rotation} \approx \eta \omega^2\ r_T^{\,2}\ \rho_{a,mean} \tag{3}$$

where η is the efficiency of compression and includes effects of friction, eddying, and so forth. The efficiency probably would be very low for the passages used in the present investigation. The efficiency may vary with cooling-air flow, but for low efficiency such variations are small. Ideally, the value of ρ used in equation (3) should be a mean value $\left(\frac{\rho_{a,H} + \rho_{a,T}}{2}\right)$. Because $\rho_{a,T}$ was not obtained in this investigation, however, $\rho_{a,H}$ was employed. This substitution can be made without excessive error if the relation between $\rho_{a,H}$ and $\rho_{a,mean}$ remains constant for a range of engine speeds and coolant weight flows, because the value of efficiency η will account to some extent for the difference between $\rho_{a,H}$ and $\rho_{a,mean}$. The $\Delta p'_{rotation}$ found in

this manner would be applicable only for similar radial coolant passages and for conditions similar to those at which the runs were made. For example, the results of this investigation, which were obtained for sea-level conditions, would not be applicable at higher altitude because the same relation between $\rho_{a,H}$ and $\rho_{a,mean}$ would not exist and the value of η would be different.

If $\Delta p'_{rotation}$ is subtracted from the total pressure in the tail cone p'_m, a pressure is obtained that can be compared with the pressure in the supply tube $p'_{a,H}$ at the turbine-rotor center line to determine how much extra pressure is required above that furnished by rotation for forcing the air through the passages. The pressure difference $p'_{a,H} - \left(p'_m - \Delta p'_{rotation}\right)$ should be a function of cooling-air flow and represents approximately the losses in a nonrotating rotor. The possibility exists that a plot of the equation

$$\frac{\rho_{a,H}}{\rho_0}\left[p'_{a,H} - \left(p'_m - \frac{\eta\omega^2 r_T^2 \rho_{a,H}}{70.7}\right)\right] = f(w_a) \qquad (4)$$

from the data for a given blade configuration with an assumed efficiency η would result in one curve for all speeds and cooling-air inlet conditions. (The term for pressure rise due to rotation in equation (4) was divided by the constant 70.7 so that the units of all the pressure terms would be consistent.) Then if the value of η for one blade was applicable to all blade configurations, the comparison method sought would be available.

This procedure was used in the present investigation; the left-hand side of equation (4) was calculated from the data and assumed values of η. The values of this parameter were then plotted against the cooling-air flow w_a.

Comparison of cooling of different blade designs. - Two methods for comparing the 15-fin-blade cooling characteristics with those of the 10-tube-blade investigation reported in reference 1 are presented. In the first method, the measured peripheral temperatures obtained in the present investigation at 10,000 rpm and at cooling-air-flow rates of 5 and 10 percent of the combustion-gas-flow rate at this speed are compared with the temperatures at comparable positions on the 10-tube blade. The 10-tube-blade temperatures were calculated from curves of φ against w_a at 10,000 rpm given in reference 1 for the same

combustion-gas and cooling-air temperatures at the blade root that existed for the 15-fin blade in the present investigation. It is impossible to compare measured temperatures in both cases because of small changes in combustion-gas and cooling-air temperatures obtained from day to day.

In the second method, the temperatures around the peripheries of both blades are compared over a range of engine speeds from 4000 to 10,000 rpm for cooling-air-flow rates of 5 and 10 percent of the gas flow obtained at each speed and for standard sea-level conditions (total temperature, 518.4° R and total pressure, 29.92 in. Hg) at the compressor inlet and in the tube supplying air on the rotor center line. The method first involved calculating the solid-blade (or effective gas temperature) and the cooling-air temperatures at the roots of both blades for these conditions. Values of the corrected combustion-gas flow $\left(w_g\sqrt{T'_{A,c,i}/518.4}\right)\Big/\left(p'_{A,c,i}/29.92\right)$, the ratio of calculated turbine-inlet total temperature to measured compressor-inlet total temperature $T'_{g,S,i}/T'_{A,c,i}$, and of the measured total-pressure ratio across the compressor $p'_{A,c,o}/p'_{A,c,i}$ were plotted against corrected engine speed $N/\sqrt{T'_{A,c,i}/518.4}$. In these parameters, pressure and temperature are in absolute units. The curves are shown in figure 6. The method of calculating $T'_{g,S,i}$ is given in reference 1. From these curves and the assumption of standard atmospheric conditions at the compressor inlet, the compressor-outlet pressure $p'_{A,c,o}$, the turbine-inlet temperature $T'_{g,S,i}$, and the combustion-gas flow rate w_g for each speed were calculated. From these values and with the method for calculating solid-blade temperatures given in reference 1, the solid-blade temperatures were calculated for the standard inlet conditions.

The temperature of the cooling air at the blade root was calculated by adding to the standard temperature at the hub, 59° F, the temperature rise from hub to root obtained from curves presented in reference 1 of measured temperature rise against w_a for several engine speeds for the conditions of speed and cooling-air flow used herein. The temperature increases obtained in the present investigation were comparable to those reported in reference 1 and consequently the curves in reference 1 could be used for both blades with very little error.

From the equation

$$T_B = T_{g,e} - \varphi\left(T_{g,e} - T_{a,e,h}\right) \tag{2a}$$

it was then possible to calculate the temperatures for both cooled blades from curves of φ against coolant flow presented herein and in reference 1 for the engine speeds and the cooling-air-flow rates assumed and the thermocouples in question.

Predictions of allowable turbine-inlet temperature. - The allowable turbine-inlet temperatures based on the measured cooling characteristics of the 15-fin blade for several conditions are given in the section "Predictions of Allowable Turbine-Inlet Temperature." The conditions for which the calculations were made are also enumerated in this section of the report. The methods for calculating these allowable turbine-inlet temperatures are explained in detail in reference 1.

RESULTS AND DISCUSSION

The results of the experimental investigation of a 15-fin air-cooled turbine blade are shown in figures 7 to 13 and are discussed in the following paragraphs.

Basic Data

Comparison of blade and cooling-air temperatures. - The results of the first series of runs to compare the temperatures of the cooling air at the root of each of the cooled blades (thermocouples E and K) and the trailing-edge temperatures common to both cooled blades (thermocouples C and I) are shown in figure 7. A 45° line has been drawn so that the data points can be compared with greater ease. Comparison of the cooling-air temperature at the root of one cooled blade (thermocouple E) with that at the root of the other cooled blade (thermocouple K) is made in figure 7(a). It can be seen that the temperature of thermocouple K compares favorably with that of E between 50° to 70° F. Below or above these values, K tends to be somewhat lower than E, with the greatest deviation being 6° F at a cooling-air temperature of 85° F. This deviation was not considered excessive and inasmuch as the blade-root cooling-air temperature is used mostly for determining the values of φ, the observed variation of cooling-air temperature would have only slight effect on the value of φ.

Comparison between the trailing-edge temperatures, which are in similar locations for both air-cooled blades (thermocouples C and I), is made in figure 7(b). It can be seen that thermocouple I is generally lower than thermocouple C with I being only about 8° F lower at the most for temperatures above 625° F. Below 625° F, thermocouple I becomes progressively lower than C, being about 20° F lower at 550° F.

This variation between the two thermocouples was not considered excessive because generally during the investigation both thermocouples were above 600° F where the difference between them is relatively small.

From these data, it was concluded that the combustion-gas flow and cooling-air flow were substantially the same through the two diametrically opposite modified cascades so that temperatures measured on one cascade could be combined with the other, for the same engine operating conditions, to determine the distribution of blade temperatures.

Effect of cooling-air flow on blade, effective gas, and cooling-air temperatures. - An example of the basic temperature data taken during the investigation is shown in figure 8 for an engine speed of 10,000 rpm. Solid-blade temperatures (or effective gas temperatures), cooled-blade temperatures, and cooling-air temperatures are plotted against cooling-air-flow rate per blade. Although cooling-air-flow rates up to approximately 0.125 pound per second per blade were passed through the blades, only data up to approximately 0.105 pound per second per blade are shown because little cooling effect was obtained for greater flow rates.

Appreciable cooling of the air-cooled blades occurred even at low air flows. The midchord temperatures (thermocouples H and J) were very cool, being generally less than one-half that of the uncooled blade for cooling-air flows per blade greater than 0.02 pound per second (fig. 8(b)). For instance, for a ratio of cooling-air flow per blade to combustion-gas flow per blade, (hereinafter designated R) of 0.05 (cooling-air flow of 0.057 lb/sec), the solid-blade temperature (thermocouple F) was 980° F and the midchord temperatures of the cooled blade (thermocouples H and J) averaged about 397° F. The leading- and trailing-edge temperatures (thermocouples G and I) were considerably higher, being about 803° and 767° F, respectively. From these results, it is apparent that the problem of reducing the leading- and trailing-edge temperatures to that of the midchord temperatures exists for the 15-fin blade as it did for the 10-tube blade configuration discussed in reference 1.

The very slight variation of the uncooled-blade temperature (thermocouple F) was caused by changes in the ambient temperature of the test cell, which in turn influenced the temperature at the turbine inlet.

In general, the cooled-blade temperatures vary as expected with changes in cooling-air flow. The leading-edge temperature (thermocouple G) is somewhat greater than the trailing edge (thermocouple I), the difference becoming less with an increase in cooling-air flow. The

cooling-air temperature at the blade root (thermocouples E and K) decreases with an increase in cooling-air flow as would be expected.

Basic temperature data are presented for an engine speed of 10,000 rpm only, because the trends of the blade, effective gas, and cooling-air temperatures at lower speeds were similar to those at 10,000 rpm.

Correlated Cooled-Blade Temperatures

According to equation (1), the temperature-difference ratio φ is approximately a function of the cooling-air flow and combustion-gas flow. Curves of φ against cooling-air flow, obtained from data similar to those shown in figure 8, are therefore presented in figure 9. Each part of figure 9 is for a particular thermocouple and includes curves for three engine speeds, and consequently three combustion-gas flows.

Except for the trailing-edge temperatures near the blade tip, figure 9(a), the data for each thermocouple could be represented by a family of curves. The values of φ generally decrease and thus the blade temperature increases with increasing engine speed. For all of the thermocouple locations except A (fig. 9(a)) and J at 10,000 rpm (fig. 9(g)), straight lines could be drawn for certain cooling-air-flow ranges that would well represent the data. For thermocouple C, the lines through the data for various engine speeds were parallel. The behavior of thermocouple A was probably caused by some characteristic of the cooling-air flow near the blade tip, and was also observed for the 10-tube configuration reported in reference 1. The relatively rapid decrease of φ with decreasing coolant flow below flow rates of about 0.02 pound per second for thermocouple J at 10,000 rpm (fig. 9(g)) was also apparent to a greater extent for the 10-tube configuration, and was verified for that configuration by applying cascade data, as explained in reference 1.

It is possible to use these curves to predict blade temperatures fairly accurately for various conditions of combustion-gas and cooling-air temperatures, cooling-air flow, and engine speed. The only known error involved is that caused by neglecting changes in the properties of the gas and air, as pointed out in reference 1.

The data results of figure 9(b) are plotted in another manner shown in figure 10. The data values of φ are divided by the measured cooling-air-flow rates raised to a power n, which is the value of the slopes in figure 9(b), and the resulting values are plotted against

the combustion-gas-flow rate for each speed. Two curves result: one for cooling-air-flow rates less than 0.018 pound per second where n is 0.08, and one for cooling-air-flow rates above 0.018 pound per second where n is 0.20. The curves fit the data quite well with several exceptions. The deviation of the line drawn through the data from the most extreme point, however, would have only a small effect on the calculated blade temperature.

In order to plot data in the manner shown in figure 10, the data must follow a trend similar to that shown in figure 9(b) for thermocouple C; that is, the resulting curves must be straight lines and parallel for each engine speed. In calculating allowable turbine-inlet temperatures for this particular blade, the calculations would have to be made for either the leading-edge or trailing-edge positions because these locations are the hottest. Fortunately, these temperatures, particularly those about 35 percent of the spanwise distance from the blade base, seem to correlate better than temperatures at other locations.

Correlated Solid-Blade Temperatures

A comparison of the calculated and the measured solid-blade or effective gas temperatures for a range of engine speeds is presented in figure 11. The calculated values of the solid-blade temperature were made by the method described in the "Calculation Procedures" section. A 45° line is drawn so that the values can be compared. The greater number of the calculated values tends to be slightly lower than the measured values with the greatest deviation being 22° F. Most of the calculated values, however, are within $\pm 10^{\circ}$ F of the measured values, and variations of this magnitude in the effective gas temperature would have very little effect on the value of cooled-blade temperatures obtained from calculated values of effective gas temperature and the curves of φ against coolant flow of figure 9.

Cooling-Air Temperature Increase through Radial Passages

The rise in the cooling-air temperature through the coolant passages leading to the base of the cooled blade in this investigation was of the same magnitude as that obtained in the investigation reported in reference 1. This similarity could be expected as the geometry of the cooling-air passages leading to the blade base was essentially the same for each investigation. Because of this similarity, curves of cooling-air temperature rise against coolant flow for various engine speeds are not presented.

Correlated Pressure Drop Required for Various Cooling-Air Flows

As previously mentioned, it was desirable that some method of evaluating the pressure drop required to force cooling air through the cooled turbine blade be available. Equation (4) was developed in the section "Calculation Procedures" for this purpose and in figure 12 the left side of equation (4) is plotted against coolant flow for the range of engine speeds investigated.

The value of η in the left side of equation (4) should be of such magnitude that

$$\frac{\rho_{a,H}}{\rho_0}\left[p'_{a,H} - \left(p'_m - \frac{\eta\omega^2 r_T^2 \rho_{a,H}}{70.7}\right)\right] = 0$$

when the weight flow is zero. A trial-and-error method was used to find the value of η and the value finally used for the data plotted in figure 12 was 0.27. Although a result of the use of this value was that the pressure-drop parameter of figure 12 became slightly negative at coolant flows below 0.01 pound per second, it resulted in the best overall correlation of pressure drop and consequently was used. Actually the value of η probably varies with coolant flow and engine speed, but it was believed that this variation would be relatively small and a constant value of η was employed.

The data correlate very well, particularly for coolant flows up to 0.05 pound per second (fig. 12). Above coolant flows of 0.05 pound per second, the data tend to scatter somewhat. Some scatter of the data is due to experimental error. The data at 4000 and 4900 rpm tend to be consistently higher than that for higher speeds, which results partly from the use of a constant value of 0.27 for η. This scatter in data was not considered excessive, however, because the error involved in computing the actual total pressure required in the hub $p'_{a,H}$ is relatively small, especially at higher engine speeds. For example, if $p'_{a,H}$ is computed on the basis of the curve presented in figure 12, the calculated value for an engine speed of 4000 rpm and a coolant flow of 0.105 pound per second is about 5.5 percent lower than the actual pressure required; at 10,000 rpm, however, the calculated value is only about 1 percent higher than the total pressure required.

The curve faired through the data points of figure 12 is plotted on logarithmic coordinates in figure 13; it results in two straight-line curves with slightly different slopes. The curve of figure 13

has a slope of 2.15 for coolant flows up to 0.09 pound per second, and for coolant flows above 0.09 pound per second the slope increases slightly to a value of 2.36.

The conclusion can be made that the pressure drop required for forcing the cooling air through the rotating passages can be satisfactorily correlated by the method evolved for this investigation. It should be noted, however, that the actual values of the pressure-drop parameter are of little significance except as a basis for comparing the cooling-air pressures required by various blade configurations having cooling air supplied to them by similar air-supply systems. The values of the pressure-drop parameter in figures 12 and 13 are quite high because of the inefficient design of the air-supply system between the measuring station in the supply tube and the base of the blade.

Termination of Investigation

The investigation of the 15-fin air-cooled blade was terminated by failure of one of the cooled blades. The failure occurred at about 10,000 rpm when the engine was being brought up to speed for a series of runs at 10,500 rpm. The blade that fractured was the one having peripheral thermocouples G, H, I, and J embedded in it. The portion of the broken blade that remained in the rotor is shown in figure 14.

At the end of the runs made at 10,000 rpm, the tail pipe was removed and the turbine blades were inspected. It was found that a crack had developed along the groove that was cut for thermocouple J. The crack was repaired by rewelding the groove. The blade was then inspected for surface cracks with a commercial fluorescent dye compound and no defects were apparent.

Inspection of the portion of the blade that remained after the failure indicated that the blade failed about 5/16 inch from the blade base, near the point where the cooling fins begin, and about 1/8 inch above the point where the weld fillet becomes tangent with the blade surface. On the convex side of the blade toward the trailing edge, the weld fillet was built up somewhat higher than for the rest of the blade and the failure path there was somewhat farther from the blade base than for the rest of the blade as can be seen from the side view of the blade in figure 14; small portions of six fins still remaining in the blade base may also be seen in this view. It appears that the failure of the blade was caused by weakening the blade near the base by cutting the grooves for the peripheral thermocouple leads and cutting slots in the blade shell for insertion of the fins. Although, as previously mentioned, inspection of the blade after repair of the

crack that developed along the groove for the lead of thermocouple J revealed no defects, it is possible that full penetration of the weld material was not obtained and that the blade was actually defective below the surface. Modification of the blade near the base would reduce the stresses in the blade at the base caused by the slots for the fins.

COMPARISON OF 15-FIN AND 10-TUBE AIR-COOLED BLADES

Geometry Factors

A comparison of the pertinent geometry factors, such as total free-flow area, inside surface area, perimeter, and hydraulic diameter of the 15-fin and 10-tube blades is made in table II. A sketch of the two blades is shown in figure 15. For the 10-tube blade the free-flow area, inside surface area, and perimeter are about 8.3, 6.3, and 6.2 percent less, respectively, than those of the 15-fin blade; the hydraulic radii of the two blades are the same. Theoretical analysis of the two blades based on these geometry factors and equation (1) of reference 1 indicated that the cooling effectiveness of the two blades would be similar; the effectiveness of the 15-fin blade would probably be slightly better.

Chordwise Temperature at Engine Speed of 10,000 rpm

A comparison of the chordwise temperatures of the 15-fin blade with those of the 10-tube blade is shown in figure 16 for an engine speed of 10,000 rpm and for R of 0.05 and 0.10. The solid line of figure 16 represents the 15-fin blade and was obtained by cross-plotting points on the curves of figure 8(b) for thermocouples G, H, I, and J (peripheral thermocouples at 35-percent span) at coolant flows of 0.057 and 0.114 pound per second (which corresponds to values of R of 0.05 and 0.10, respectively, for the 15-fin blade). The solid-line curves were then faired through these points for thermocouples G, H, and I in figure 16(a) and for thermocouples G, J, and I in figure 16(b). Because this procedure established only three points for the chordwise temperature distribution, unpublished cascade data based on more data points were used as a guide in drawing the curves for figure 16. Temperatures for the 10-tube blade (dashed curve in fig. 16) were computed by employing equation (2a).

The values of effective gas temperature $T_{g,e}$ and cooling-air temperature $T_{a,e,h}$ for substitution in equation (2a) were obtained from figure 16 at cooling-air-flow rates of 0.057 and 0.114 pound per second. Values of φ were obtained from figure 13 of reference 1 at cooling-air-flow rates equivalent to coolant- to combustion-gas-flow ratios of 0.05 and 0.10 for that investigation. The resulting coolant flows were 0.057 and 0.114 pound per second, which were the same for this investigation and that of reference 1 because the combustion-gas flows for both investigations were nearly equal. By employing this procedure, the blade temperatures of the 15-fin and 10-tube blades were compared at the same conditions.

From figure 16 it can be seen that the temperatures of the 15-fin blade near the midchord are appreciably lower than those of the 10-tube blade, especially for thermocouple J, figure 16(b). At $R = 0.05$, for example, the 15-fin blade for thermocouple J is 104° F cooler than the 10-tube blade (357° F compared with 461° F); the corresponding solid-blade temperature was 980° F and the cooling-air temperature at the blade root was 70° F. At $R = 0.10$, thermocouple J of the 15-fin blade was 96° F cooler (297° F compared with 393° F). For thermocouple position H (fig. 16(a)), the 15-fin blade was about 70° and 55° F cooler than the 10-tube blade at ratios of coolant flow to combustion-gas flow of 0.05 and 0.10, respectively.

At a point near the leading edge (thermocouple G), the 10-tube blade was 13° F cooler (789° F compared with 802° F) and 35° F cooler (697° F compared with 732° F) at $R = 0.05$ and 0.10, respectively. Near the trailing edge (thermocouple I), the 15-fin blade was 48° F cooler than the 10-tube blade for both values of R, that is, 767° F and 740° F for the 15-fin blade and 815° F and 788° F for the 10-tube blade at $R = 0.05$ and 0.10, respectively.

Although the 15-fin blade reduced the midchord temperatures appreciably, as compared with those of the 10-tube blade, the temperatures at the leading and trailing edges for both blades were quite similar. This result indicates that further research is necessary to obtain cooled-blade configurations that will produce more effective cooling at the leading and trailing edges.

Effect of Engine Speed on Chordwise Temperature for Standard Engine-Inlet Conditions

Effective gas and blade cooling-air temperatures at various engine speeds. - The variation in effective gas temperature and effective blade-cooling-air temperature with engine speed for standard atmospheric conditions at the engine inlet is shown in figure 17. These curves were plotted from calculations made according to the method described in the "Calculation Procedures" section. The effective gas temperature (fig. 17(a)) decreases about 70° F (from 943° to 873° F) with increasing engine speed up to an engine speed of about 8000 rpm; the greater part of the decrease occurs between 4000 and 5000 rpm. Above 8000 rpm, the effective gas temperature rapidly rises to a value of about 1000° F at 10,000 rpm. Curves of the variation of effective cooling-air temperature with engine speed are shown in figure 17(b) for cooling-air-flow rates of 5 and 10 percent of the combustion-gas flow. The cooling-air temperature rises slowly for engine speeds up to about 8000 rpm and then rises quite rapidly for speeds above 8000 rpm.

Comparison of blade temperatures over range of engine speeds. - Comparisons of the temperatures of thermocouple positions G, H, I, and J (peripheral thermocouples) for the 15-fin and 10-tube blades for values of R of 0.05 and 0.10 over a range of engine speeds are made in figure 18. The temperatures in figure 18 were computed by employing the effective gas and blade-cooling-air temperatures of figure 17 in equation (2a). The values of φ from data presented in this report and reference 1 were employed in equation (2a) for each engine speed, thermocouple location, and cooling-air to gas-flow ratio, as discussed in the "Calculation Procedures" section.

For thermocouple position G (leading edge), the two blade temperatures are quite similar as shown in figure 18(a), with the 15-fin blade being hotter than the 10-tube blade at engine speeds below about 5000 rpm and above 9000 rpm. For engine speeds between about 5000 and 7000 rpm, the temperatures are practically the same; between about 7000 and 9000 rpm, the 15-fin blade is cooler with the maximum difference between the two configurations occurring at about 8000 rpm.

For thermocouples H (midchord) and I (trailing edge) (figs. 18(b) and 18(c), respectively), the 15-fin blade is consistently cooler throughout the entire speed range; thermocouple H is a minimum of about 30° F cooler and a maximum of about 97° F cooler. For thermocouple I, the curves for the two blades nearly parallel one another,

with the 15-fin blade 25° to 35° F cooler than the 10-tube blade throughout most of the speed range.

For thermocouple J (midchord), figure 18(d), the 15-fin blade is generally about 40° to 65° F cooler than the 10-tube blade for engine speeds up to about 6500 rpm. Above 6500 rpm, the temperature of the 10-tube blade increases rapidly until a maximum temperature is reached at an engine speed of about 9000 rpm. At this speed the 15-fin blade is then about 177° F and 190° F cooler than the 10-tube blade at coolant- to gas-flow ratios of 5 and 10 percent, respectively. At 10,000 rpm, the temperature of the 10-tube blade has decreased considerably and the 15-fin blade is about 90° F cooler than the 10-tube blade.

In general, the temperature patterns of the 15-fin blade in figure 18 follow the same trend as that of the effective gas temperature of figure 17(a); that is, the blade temperature decreased from engine speeds of 4000 to about 5000 rpm, was relatively flat between about 5000 and 8000 rpm, and then increased with further increase in speed. The patterns for the 10-tube blade were quite similar to those of the 15-fin blade except for thermocouple J, which behaved peculiarly at engine speeds above about 6500 rpm. The behavior of thermocouple J for the 10-tube blade is discussed in reference 1.

PREDICTIONS OF ALLOWABLE TURBINE-INLET TEMPERATURE

Conditions and Assumptions for Calculations

Calculations of the allowable turbine-inlet temperature were made considering blades made of two materials, one with a low critical alloy content (Timken alloy 17-22A, which has 1.29 percent chromium, 0.52 percent molybdenum, and 0.25 percent vanadium) and a high-temperature alloy, X-40. The first material has a low strategic metal content and consequently satisfies the first objective set forth in the "Introduction," namely, to obtain cooled turbine-blade configurations of nonstrategic blade materials that will permit operation of the engine at current turbine-inlet temperatures.

Further conditions of the calculations were for design engine speed of 11,500 rpm, a coolant flow equivalent to 5 percent of the combustion-gas flow, standard sea-level atmospheric conditions at the engine inlet, cooling air bled directly from the compressor, and a blade-fabrication method in which the fins were supported by the blade shell and the blade shell in turn was supported by the base. The method of determining the cooling-air temperature, allowable turbine-inlet temperature, and so forth is given in detail in reference 1.

Because the engines employed for both the 15-fin- and 10-tube-blade investigations had essentially the same compressor temperature-rise characteristics, the same value of the cooling-air temperature at the blade root as determined in reference 1 (namely, 506° F) was used.

In addition, the calculations were made on the basis of the trailing-edge temperatures being the limiting condition and also on the basis that the entire blade cooled as well as the midchord of the blade, as indicated by thermocouple J. For this last condition, it was assumed that the temperature distribution of the blade from hub to tip was the same at the midchord as at the trailing edge. Only the simple centrifugal blade stresses due to rotation were considered; the vibratory and thermal stresses were neglected.

In general, these conditions are the same as those employed for part of the allowable turbine-inlet calculations made for the 10-tube blade in reference 1 and permit direct comparison of the allowable turbine-inlet temperatures of the 15-fin and 10-tube blades.

Allowable Temperatures

Allowable temperatures for nonstrategic metal. - A summary of the results of calculations of the allowable turbine-inlet temperatures for the conditions specified are shown in table III. The results of similar calculations made for the 10-tube blade of reference 1 are also shown for purposes of comparing results of the two blade configurations. For a nonstrategic metal on the basis of trailing-edge temperatures, the allowable turbine-inlet temperature was 1381° F for the 15-fin blade as compared to 1370° F for the 10-tube blade. Although the temperatures and stresses in the 15-fin blade were somewhat less than those of the 10-tube blade, the allowable metal temperature for the 17-22A alloy changes little within the stress range being considered; consequently the allowable turbine-inlet temperature is essentially the same for the two blades when based on the trailing-edge temperatures. When the allowable turbine-inlet temperature is based on the midchord temperature of thermocouple J, however, the allowable turbine-inlet temperature for the 15-fin blade is about 2372° F as compared with 2090° F for the 10-tube blade. This increase in allowable gas temperature of 282° F for the 15-fin blade over that of the 10-tube blade results from the midchord temperature of the 15-fin blade being considerably lower than that of the 10-tube blade, as evidenced in figures 16(b) and 18(d).

Allowable temperatures for a high-temperature alloy. - The calculated allowable turbine-inlet temperature for the 15-fin and 10-tube

blades when made of a high-temperature alloy, X-40, which contains large amounts of critical alloys, is also shown in table III. The allowable temperature at the turbine inlet based on trailing-edge temperatures of the 15-fin blade is about 1813° F compared with 1615° F for the 10-tube blade, an increase of 198° F. When based on thermocouple J at the midchord, the allowable inlet temperatures are above 3000° F for the 15-fin blade and about 2600° F for the 10-tube blade. When a high-temperature alloy is employed, it is apparent that the 15-fin blade would permit significant increases of the turbine-inlet temperature over those allowable for the 10-tube blade, even when based on the trailing-edge temperatures.

SUMMARY OF RESULTS

The results of an investigation conducted to determine experimentally the effectiveness of air-cooling several turbine blades in a turbojet engine are presented for a hollow blade shell with 15 fins inserted.

1. The 15-fin blade cooled appreciably better than the 10-tube blade at a point near the midchord. For example, at an engine speed of 10,000 rpm, a cooling-air temperature at the blade root of 70° F, a ratio of coolant flow to combustion-gas flow of 0.05, and an effective gas temperature (or solid-blade temperature) of 980° F, the temperature on the convex side of the 15-fin blade was about 104° F lower than that of the 10-tube blade (357° F compared with 461° F), whereas the temperature on the concave side of the blade was about 70° F lower. For points near the leading and trailing edges of the blades, the temperatures at the given operating conditions were quite similar for the 15-fin and 10-tube blades. The temperatures near the leading and trailing edges of the 15-fin blade were about 13° F hotter (802° F compared with 789° F) and 48° F cooler (767° F compared with 815° F), respectively, than those of the 10-tube blade.

2. A method of correlating the pressure drop required for forcing cooling air through the rotating passages for any engine speed and coolant flow was developed so that the pressure drop for various blade configurations can be evaluated.

3. On the basis of the trailing-edge temperatures obtained on the blades in this investigation, calculations showed that turbine-inlet temperatures of 1381° F possibly could be obtained at design speed with a nonstrategic metal, Timken alloy 17-22A, assuming standard sea-level compressor-entrance conditions, cooling air bled off at the exit of the

compressor, a coolant flow 5 percent of the gas flow, and with a blade-fabrication method such that the fins and the shell are both supported by the base.

4. For the same conditions, but assuming that the entire blade cools chordwise as well as the midchord of the blade and that the same temperature distribution from the hub to the tip of the blade exists at the midchord, the calculations indicated that the allowable turbine-inlet temperature of 1381° F could be increased to about 2372° F.

5. For the same engine conditions mentioned and for a high-temperature alloy, X-40, the allowable turbine-inlet temperature would be approximately 1813° F when based on the trailing-edge temperatures. When based on the midchord temperature, the inlet temperature could be increased to a value above 3000° F.

Lewis Flight Propulsion Laboratory,
National Advisory Committee for Aeronautics,
Cleveland, Ohio, August 1, 1950.

REFERENCES

1. Ellerbrock, Herman H., Jr., and Stepka, Francis S.: Experimental Investigation of Air-Cooled Turbine Blades in Turbojet Engine. I - Rotor Blades with 10 Tubes in Cooling-Air Passages. NACA RM E50I04,

2. Livingood, John N. B., and Brown, W. Byron: Analysis of Spanwise Temperature Distribution in Three Types of Air-Cooled Turbine Blade. NACA Rep.

3. Ellerbrock, Herman H., Jr., and Ziemer, Robert R.: Preliminary Analysis of Problem of Determining Experimental Performance of Air-Cooled Turbine. III - Methods for Determining Power and Efficiency. NACA RM E50E18, 1950.

4. Ellerbrock, Herman H., Jr., and Ziemer, Robert R.: Preliminary Analysis of Problem of Determining Experimental Performance of Air-Cooled Turbine. I - Methods for Determining Heat-Transfer Characteristics. NACA RM E50A05, 1950.

EXPERIMENTAL INVESTIGATION OF AIR-COOLED TURBINE BLADES IN A TURBOJET ENGINE

II - ROTOR BLADES WITH 15 FINS IN COOLING-AIR PASSAGES

Robert O. Hickel,
Aeronautical Research
Scientist.

Herman H. Ellerbrock, Jr.,
Aeronautical Research
Scientist.

Approved:
Oscar W. Schey,
Aeronautical Research
Scientist.

mch

TABLE I - ENGINE OPERATING CONDITIONS

Series	Nominal engine speed N (rpm)	Average compressor-inlet condition		Thermocouple group	Combustion gas flow w_g (lb/sec)	Fuel flow w_f (lb/sec)	Cooling-air flow per blade w_a (lb/sec)	Cooling-air inlet temperature $T_{a,H}$ (°F)	Cooling-air temperature, blade root $T_{a,e,h}$ (°F)	Calculated turbine-inlet total temperature $T'_{g,S,i}$ (°F)
		Pressure $p'_{A,c,i}$ (in. Hg)	Temperature $T'_{A,c,i}$ (°F)							
1	4000	29.0	46-54	C,E,I,K	20.8-21.2	0.303-0.304	0.005-0.123	53-70	56-94	911-914
2	4000	29.43	40-42	A,C,D,E,L	20.8-21.6	.303- .304	.006- .125	53-70	50-84	905-919
3	4000	29.56	50-52	G,H,I,J,K,F	20.4-20.7	.306- .308	.005- .124	50-76	53-99	931-946
4	4900	29.39	37-40	A,C,D,E,L	26.3-27.2	.359- .361	.005- .126	38-62	44-87	880-900
5	4900	28.10	53-63	G,H,I,J,K,F	24.1-25.1	.324- .357	.005- .129	47-64	61-97	940-967
6	5400	29.63	51-63	A,C,D,E,F	27.8-28.7	.370- .371	.005- .124	52-68	61-96	946-950
7	5400	29.62	44-46	G,H,I,J,K,F	28.8-29.2	.372- .373	.005- .125	44-62	54-91	930
8	6000	29.44	47-48	A,C,D,E,F	32.2-32.7	.414- .415	.006- .125	42-62	56-96	907-949
9	6000	29.64	45-56	G,H,I,J,K,F	32.5-33.7	.412- .415	.005- .106	46-66	57-96	936-948
10	8000	29.52	37-38	A,C,D,E,F	47.0-47.9	.536- .548	.006- .124	41-60	61-98	944-973
11	8000	29.93	43-45	G,H,I,J,K,F	46.0	.534- .539	.006- .126	41-61	58-101	966-968
12	9000	29.63	37-40	A,C,D,E,F	54.1-54.5	.635- .636	.006- .124	44-68	65-106	1025
13	9000	29.46	39-43	G,H,I,J,K,F	53.7-54.8	.625- .630	.006- .126	40-68	63-117	1032-1036
14	10,000	29.42	45-52	A,C,D,E,F	61.8-62.9	.796- .802	.008- .125	51-68	68-125	1158-1167
15	10,000	29.63	42-47	G,H,I,J,K,F	61.6-62.2	.792- .795	.008- .123	51-70	69-135	1155-1163

NACA

TABLE II - COMPARISON OF GEOMETRY FACTORS

FOR 15-FIN AND 10-TUBE BLADES

Geometry factor	15-fin blade	10-tube blade
Total free-flow area of cooling-air passages (sq in.)	0.24	0.22
Total inside surface area exposed to cooling air, (sq in.)	38.1	35.7
Total perimeter of cooling-air passages (in.)	9.7	9.1
Hydraulic diameter (in.)	0.10	0.10

TABLE III - COMPARISON OF PREDICTED ALLOWABLE TURBINE-INLET TEMPERATURES FOR 15-FIN AND 10-TUBE BLADES

[Engine speed, 11,500 rpm; cooling-air-flow rate, 5 percent of combustion-gas-flow rate, standard sea-level atmospheric conditions at engine inlet; blade shell supporting fins or tubes and base supporting shell]

Blade configuration	Allowable turbine-inlet temperature, °F			
	Timken alloy, 17-22A		High-temperature alloy, X-40	
	Based on trailing-edge-temperature distribution	Based on midchord temperature	Based on trailing-edge-temperature distribution	Based on midchord temperature
15 fin	1381	2372	1813	above 3000
10 tube	1370	2090	1615	2600

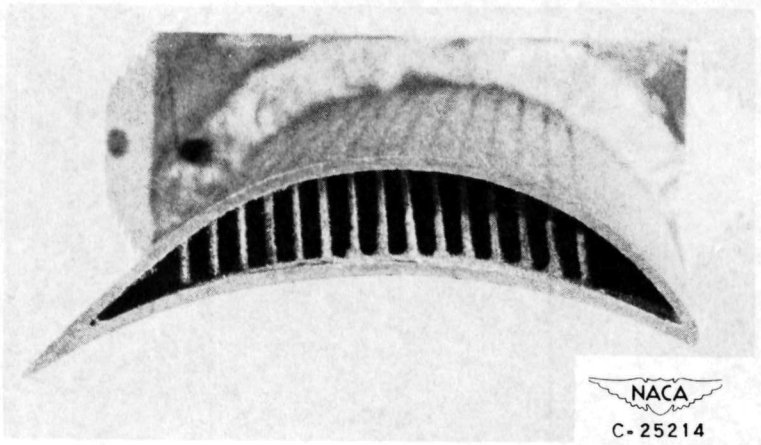

(a) Top view of blade.

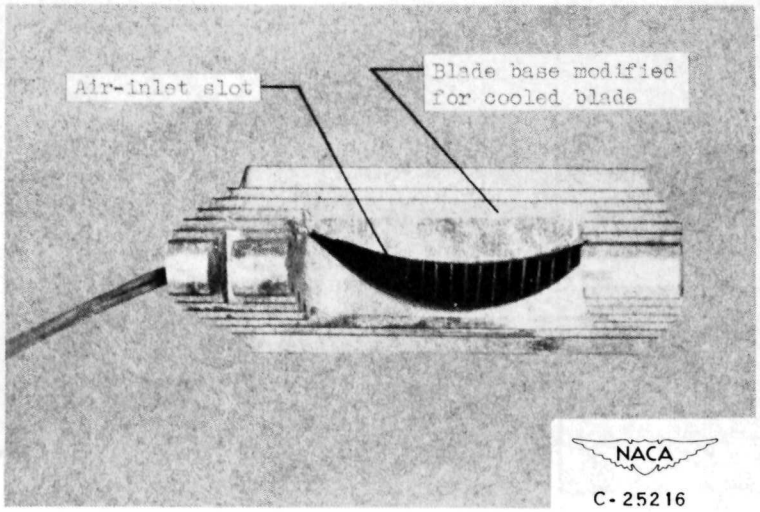

(b) Base view of blade.

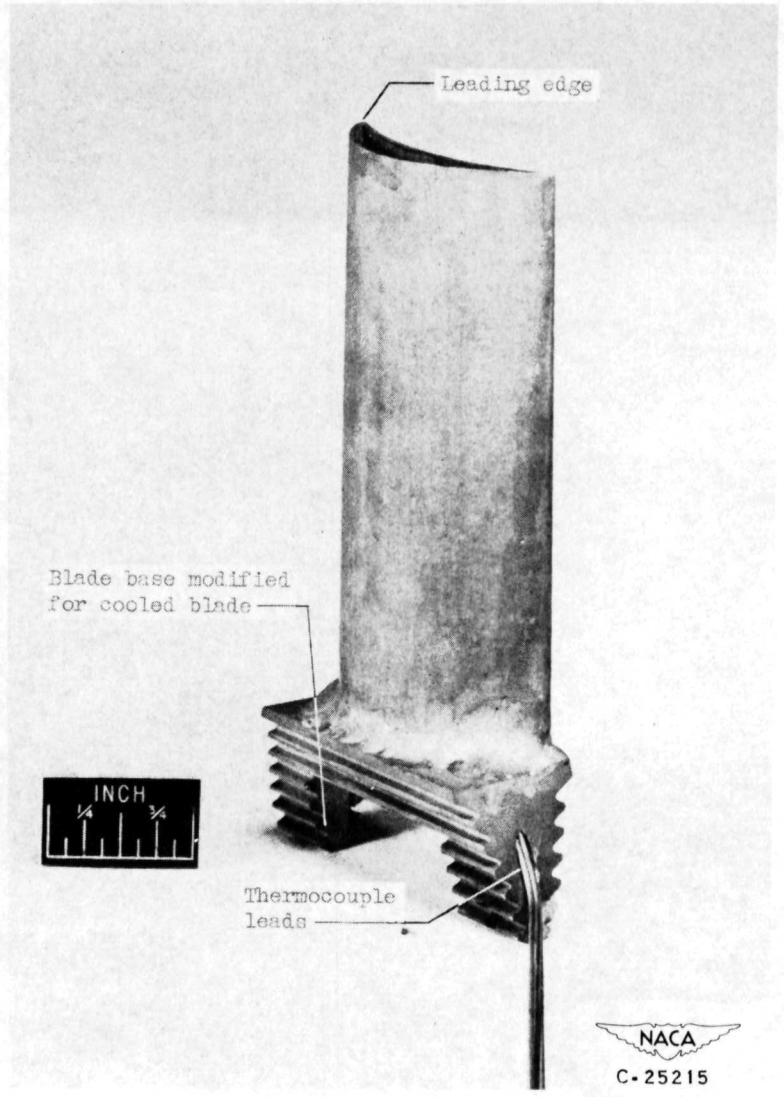

(c) Side view of blade.

Figure 1. - Cooled turbine blade with 15 fins.

"Page missing from available version"

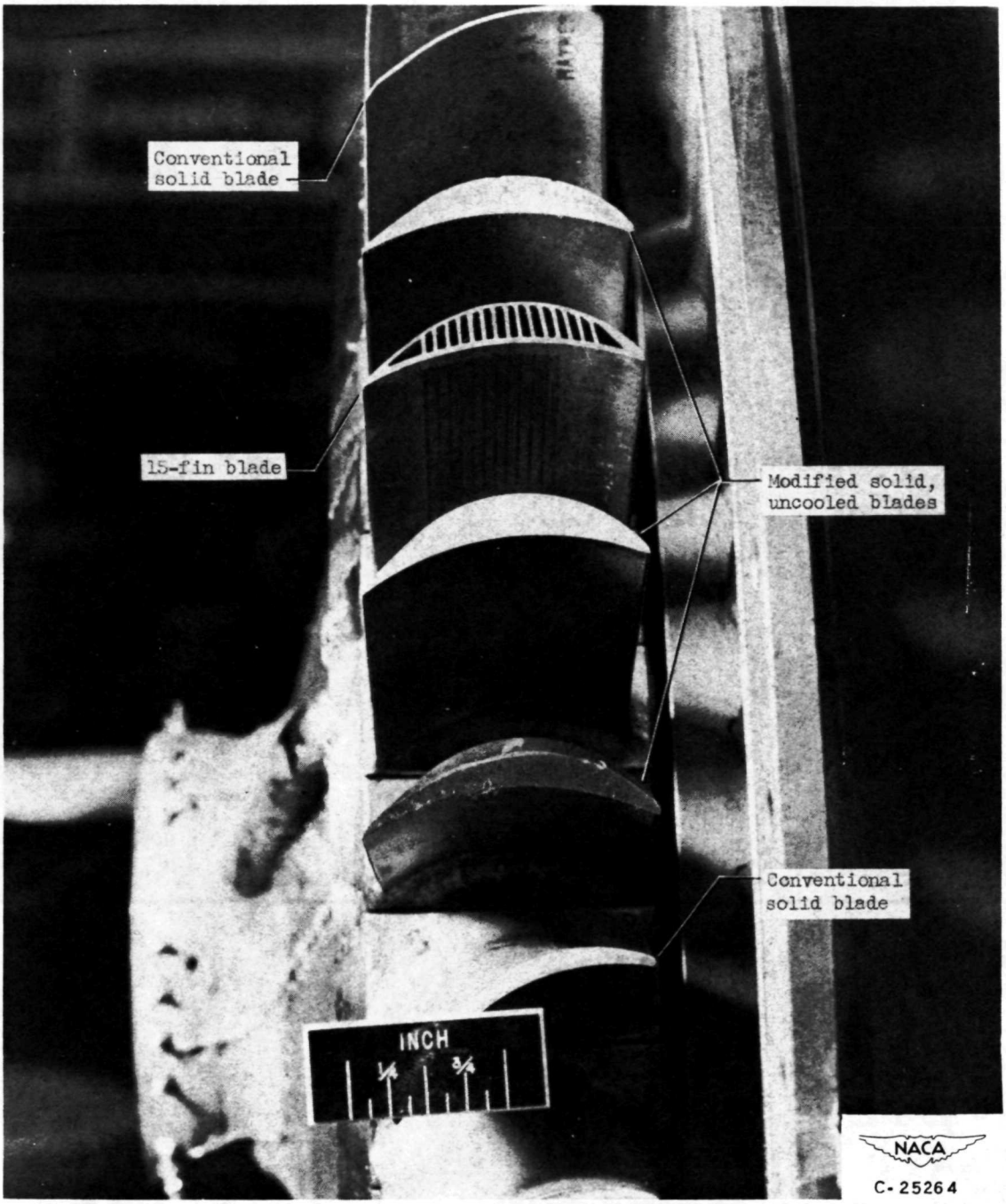

Figure 2. - Arrangement of modified turbine blades in turbine rotor.

"Page missing from available version"

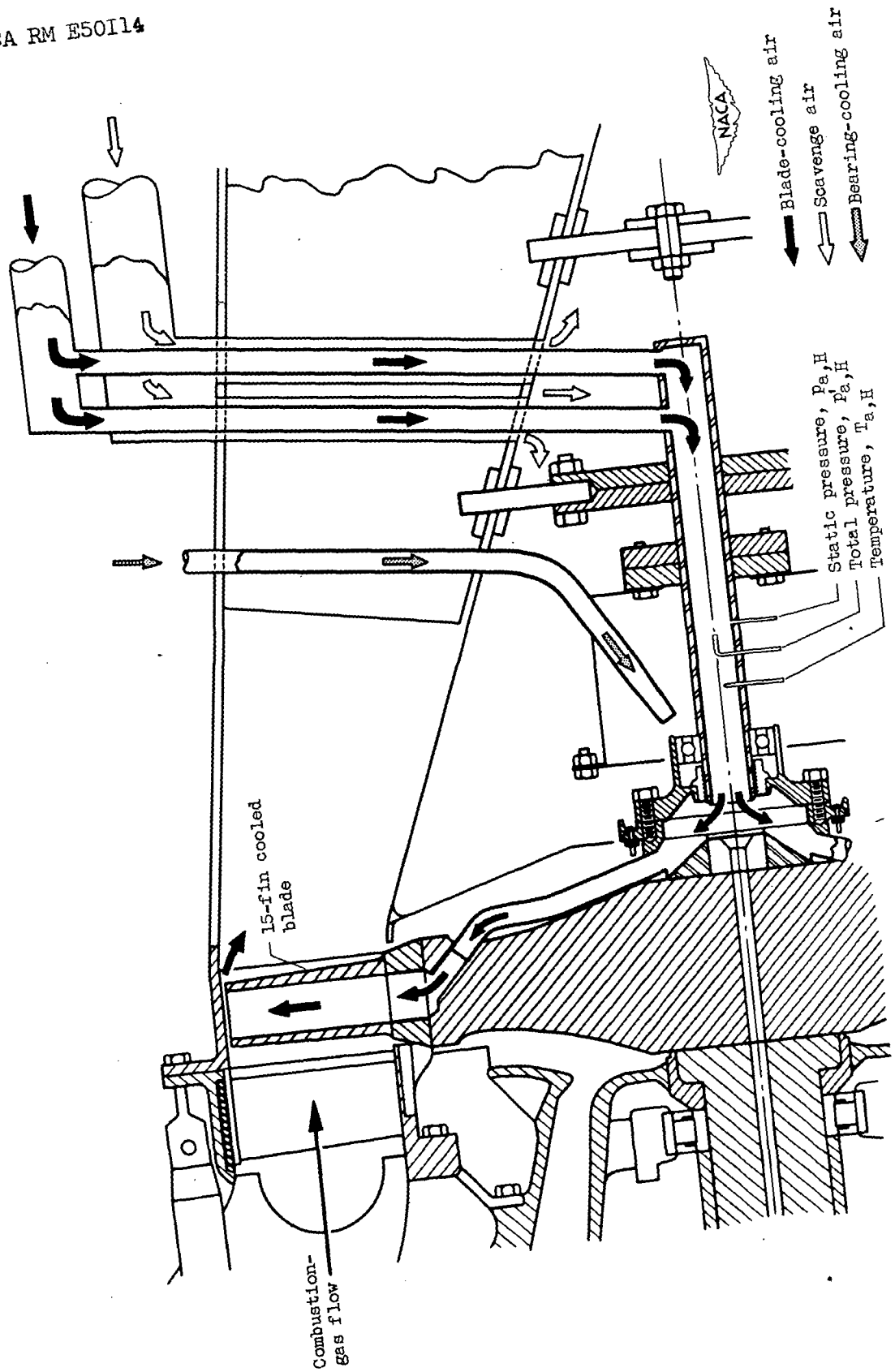

Figure 3. - Location of cooling-air instrumentation in tail cone.

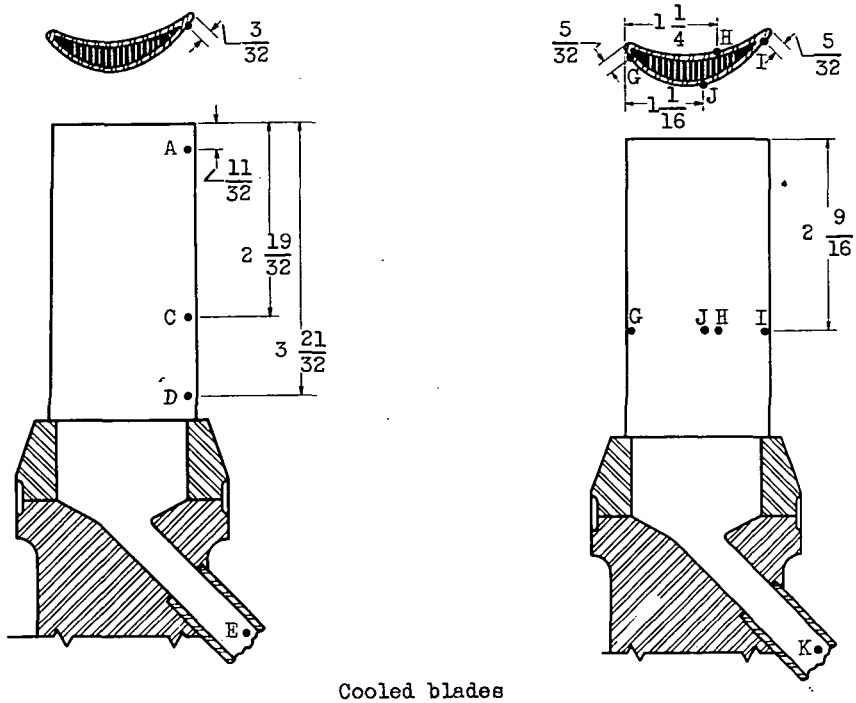

Cooled blades

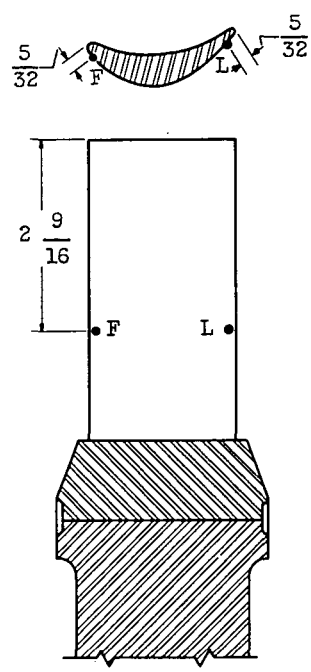

Uncooled blade

Figure 4. - Schematic diagram of thermocouple locations on cooled and uncooled blades. (All dimensions in inches.)

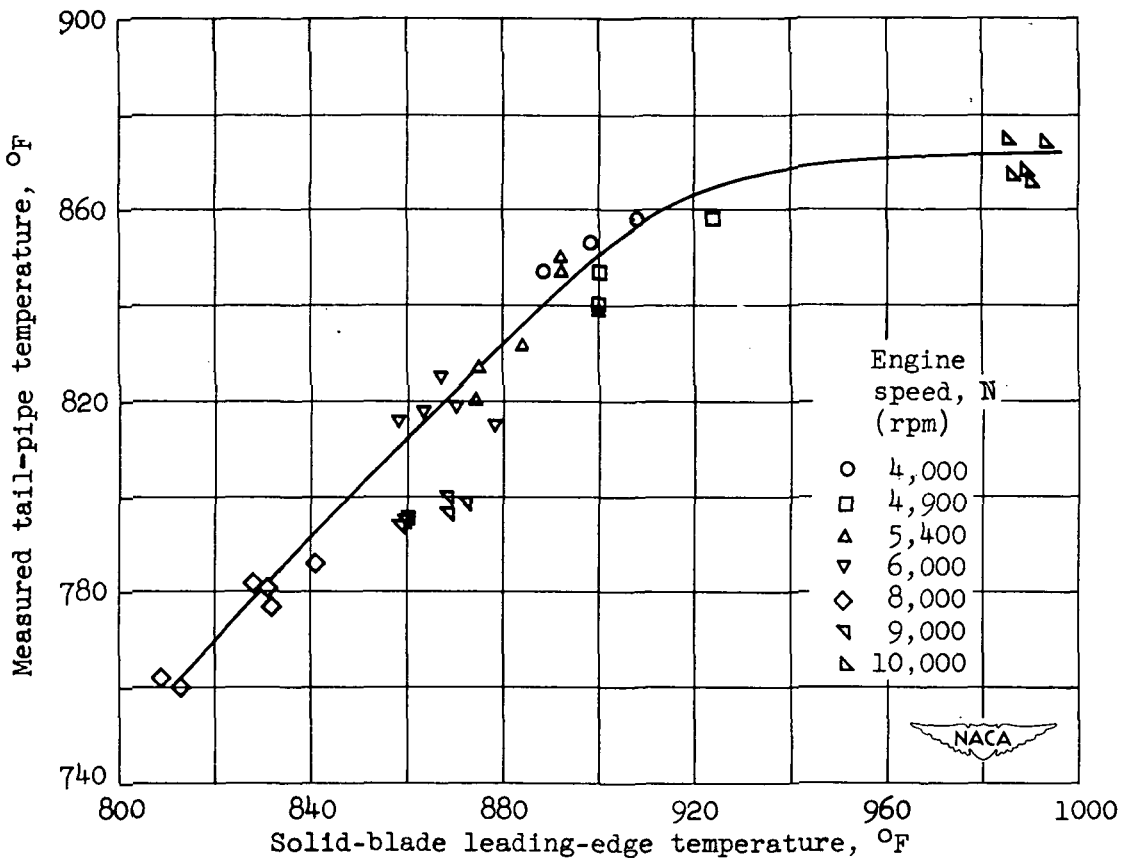

Figure 5. - Variation of solid-blade temperature with measured tail-pipe temperature.

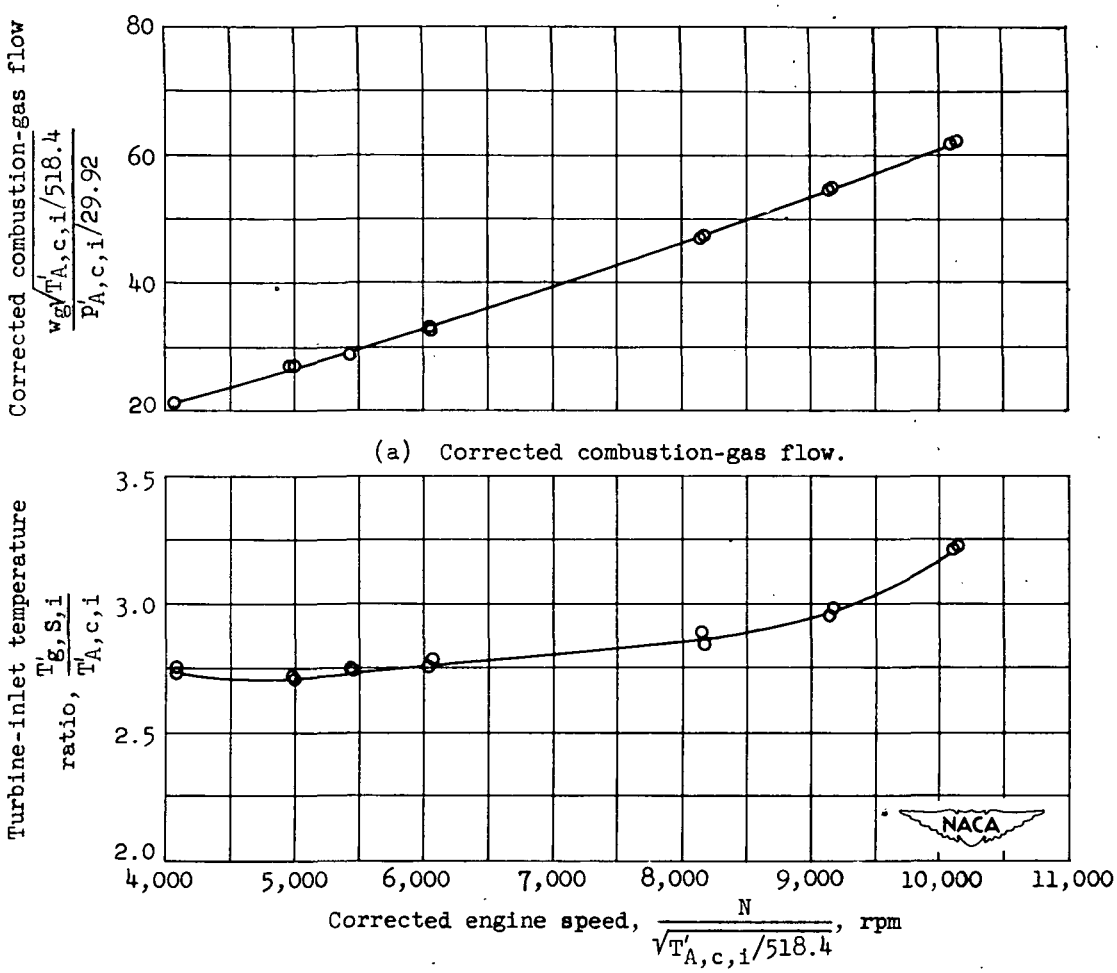

(a) Corrected combustion-gas flow.

(b) Turbine-inlet temperature ratio.

Figure 6. - Correlation of engine operating conditions.

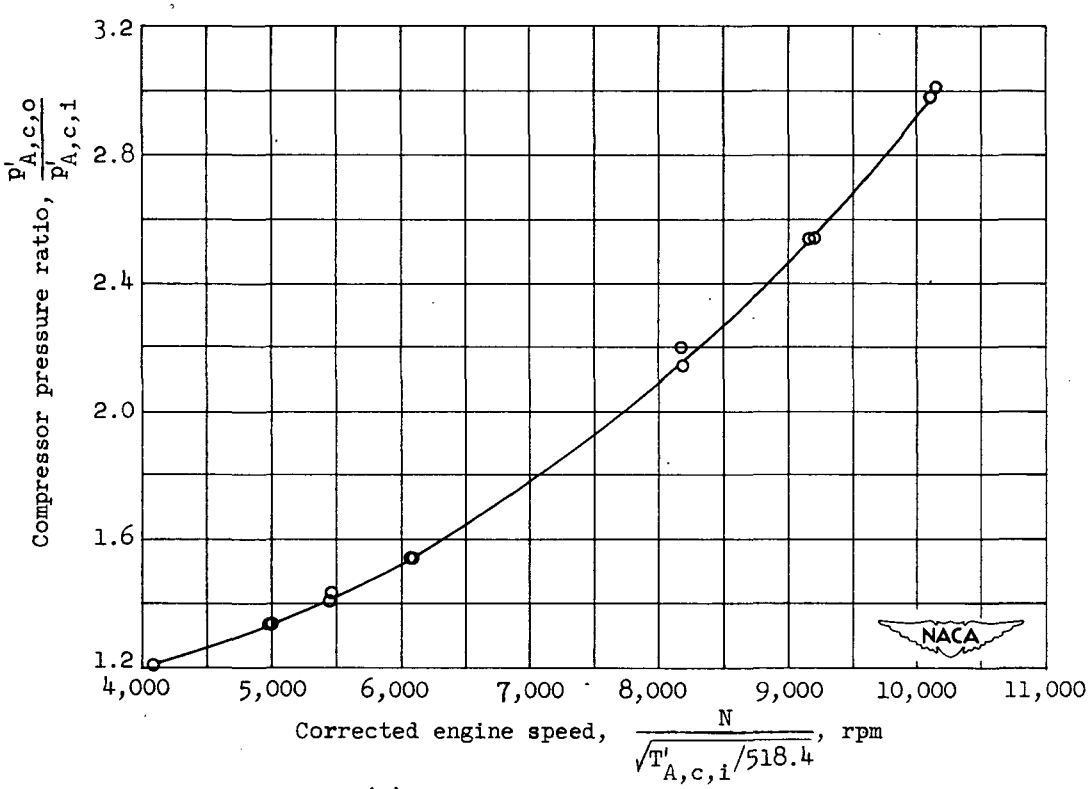

(c) Compressor pressure ratio.

Figure 6. - Concluded. Correlation of engine operating conditions.

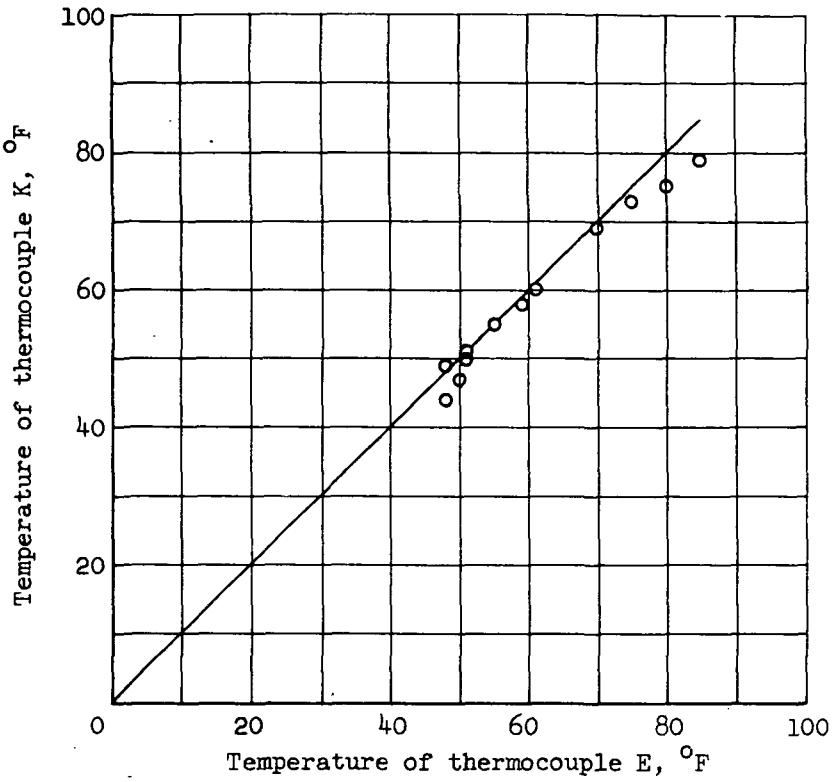

(a) Cooling-air temperature at blade root.

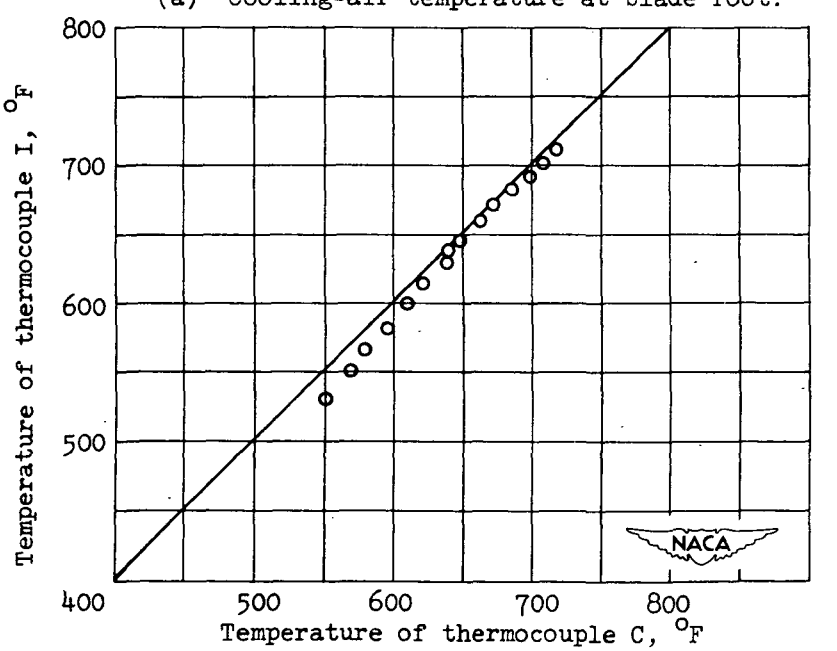

(b) Trailing-edge temperature.

Figure 7. - Comparison of temperatures at similar locations.

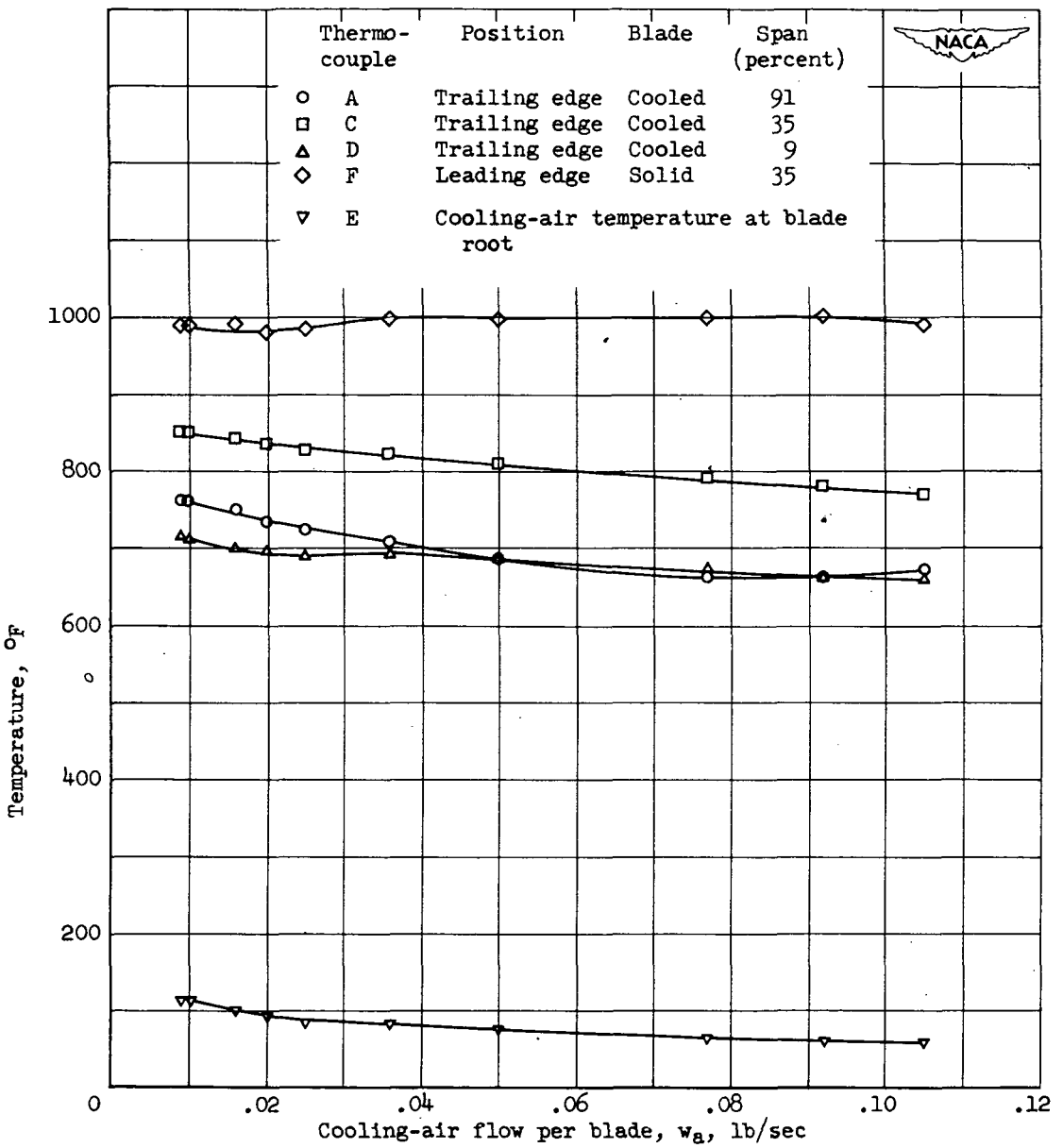

(a) Series 14.

Figure 8. - Effect of cooling-air-flow rate on modified-blade and cooling-air temperatures at engine speed of 10,000 rpm.

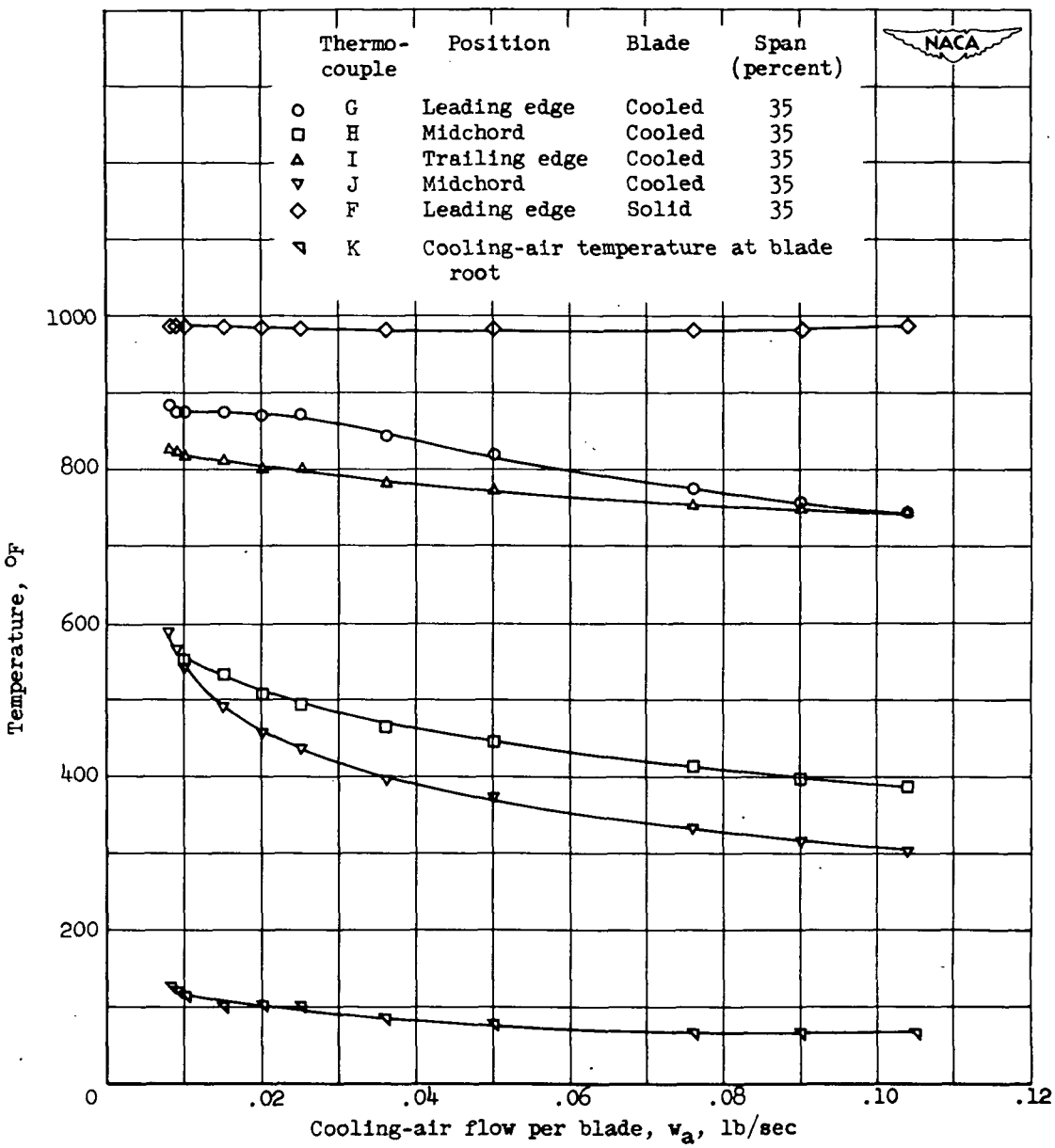

(b) Series 15.

Figure 8. - Concluded. Effect of cooling-air-flow rate on modified blade and cooling-air temperatures at engine speed of 10,000 rpm.

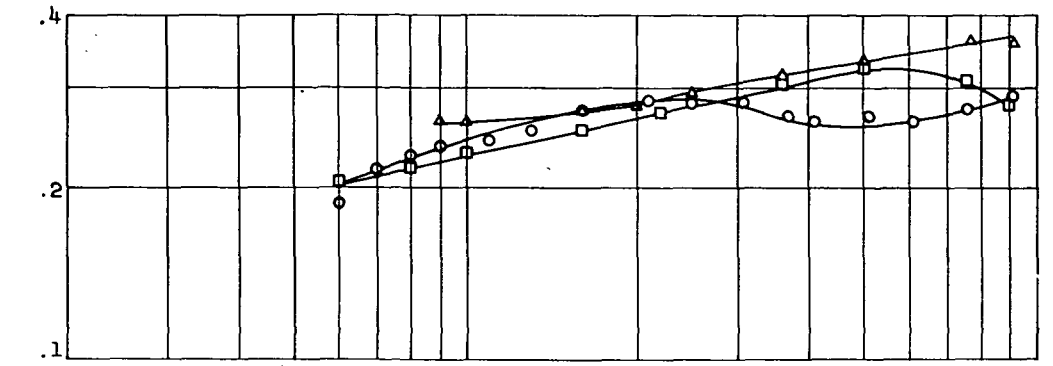

(a) Thermocouple A (trailing edge, 91-percent span).

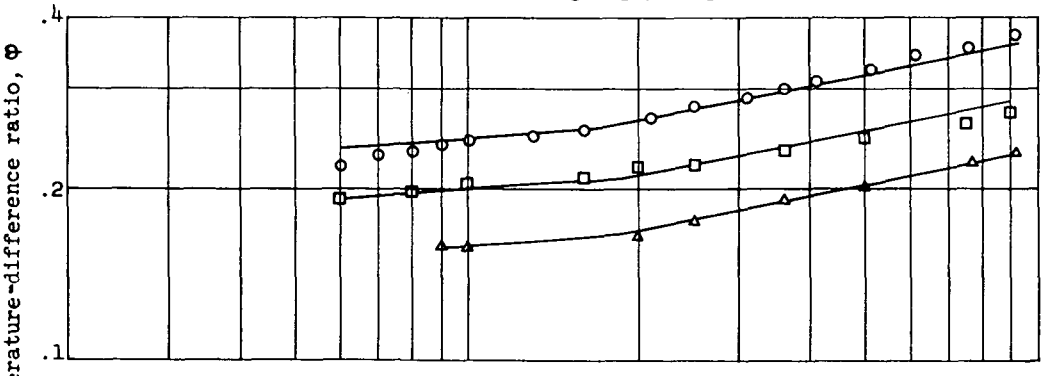

(b) Thermocouple C (trailing edge, 35-percent span).

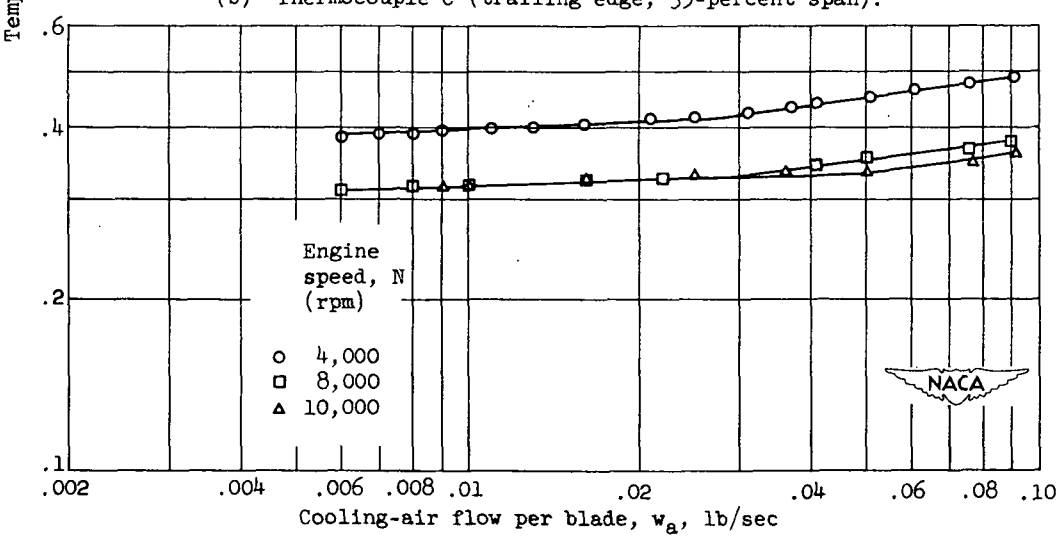

(c) Thermocouple D (trailing edge, 9-percent span).

Figure 9. - Effect of cooling-air flow on temperature difference ratio for several engine speeds.

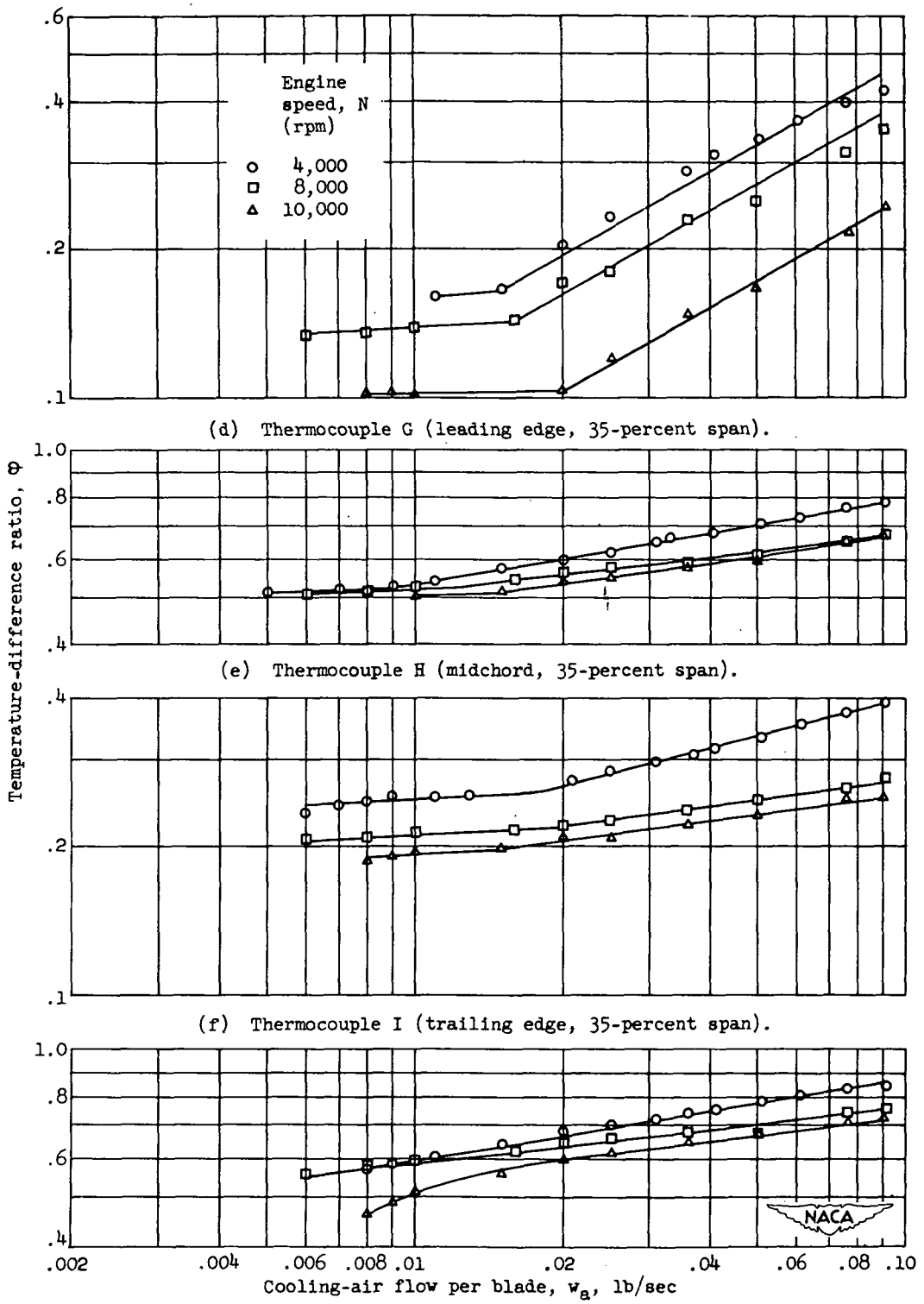

(d) Thermocouple G (leading edge, 35-percent span).

(e) Thermocouple H (midchord, 35-percent span).

(f) Thermocouple I (trailing edge, 35-percent span).

(g) Thermocouple J (midchord, 35-percent span).

Figure 9. - Concluded. Effect of cooling-air flow on temperature difference ratio for several engine speeds.

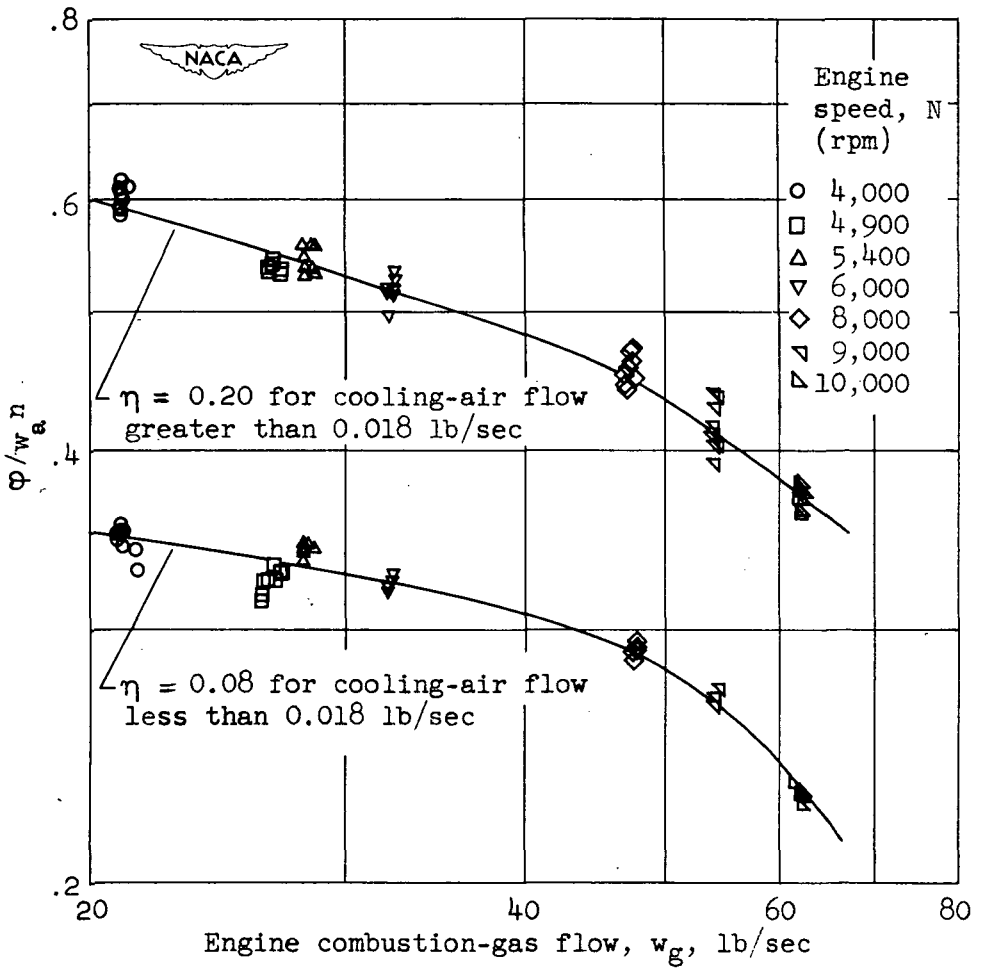

Figure 10. - Variation of φ/w_a^n ratio with engine combustion-gas flow for thermocouple C (trailing edge, 35-percent span).

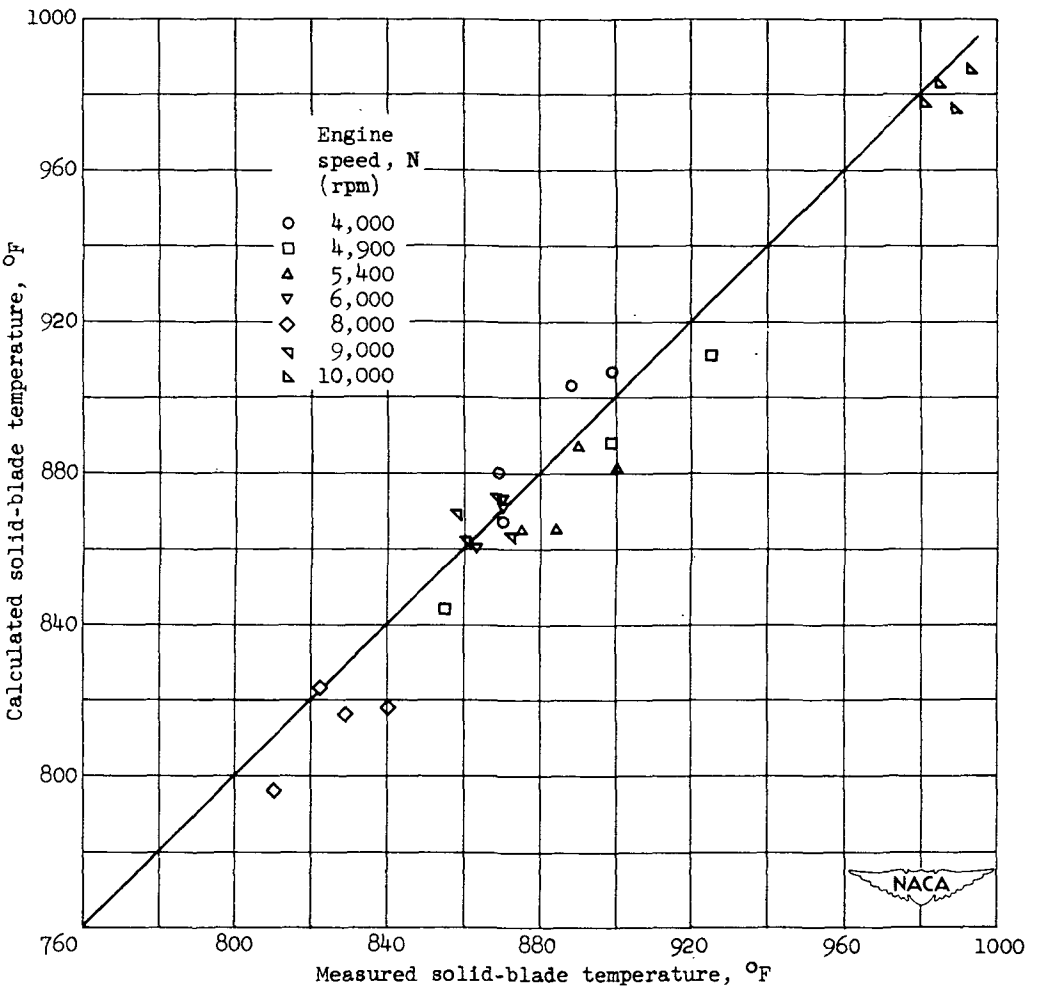

Figure 11. - Comparison of calculated and measured solid-blade temperatures.

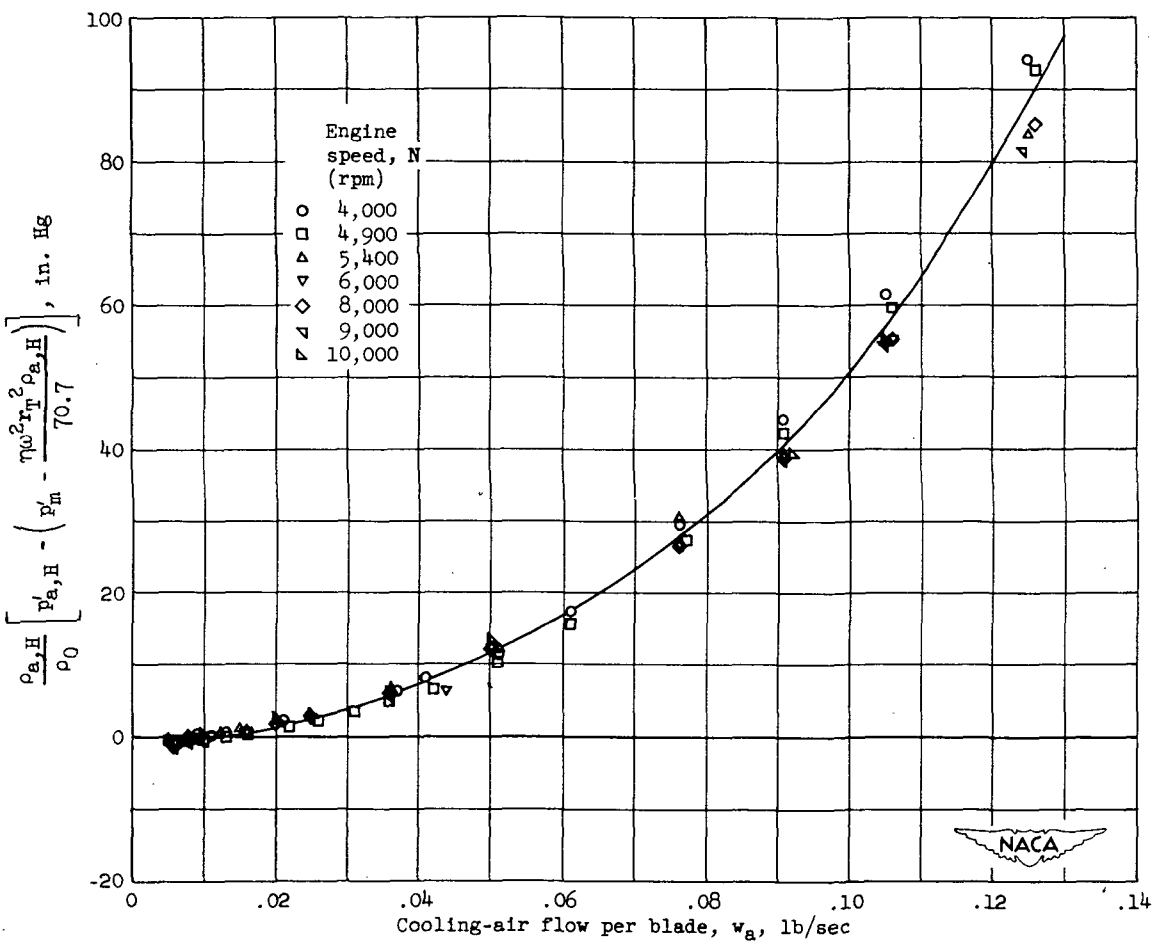

Figure 12. - Correlation of cooling-air-pressure data.

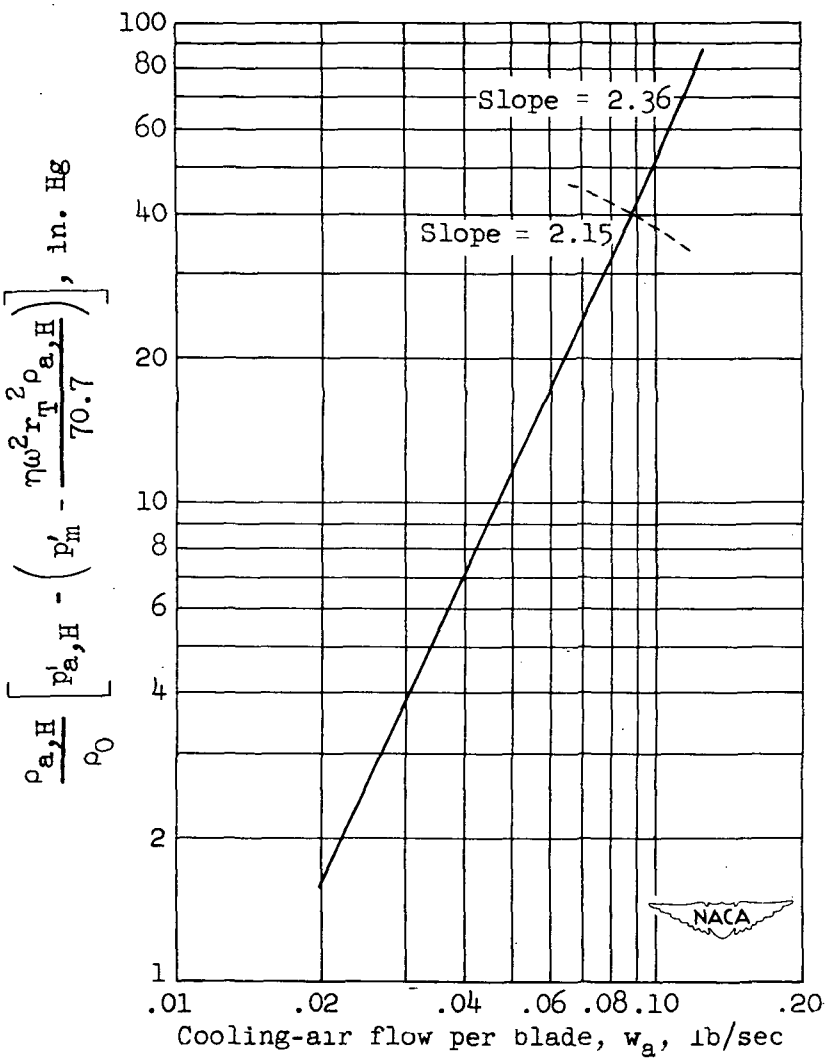

Figure 13. - Final cooling-air-pressure correlation curve.

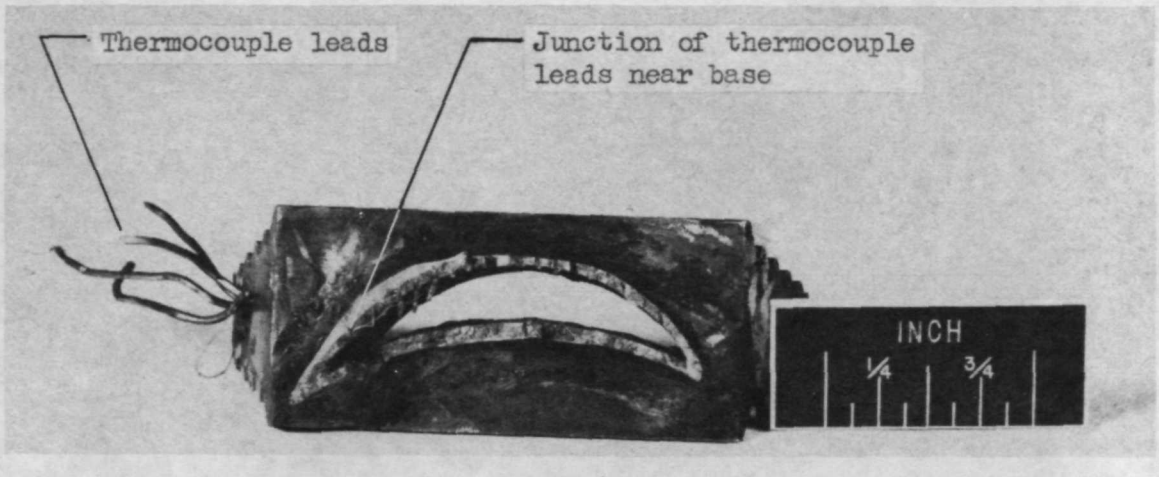

Top view.

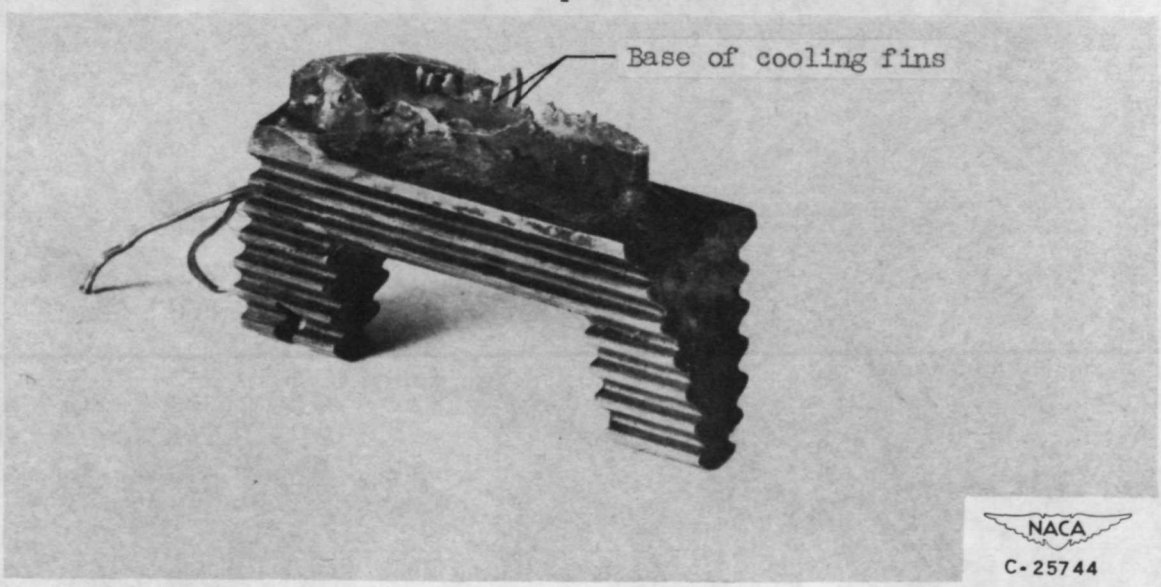

Side view.

Figure 14. - Failure path along fractured blade.

"Page missing from available version"

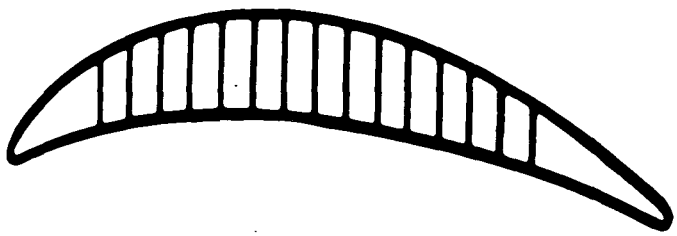

(a) 15-fin blade.

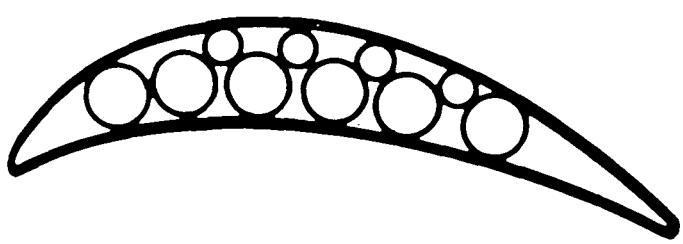

(b) 10-tube blade.

Figure 15. - Schematic diagram of cross section of 15-fin and 10-tube blades.

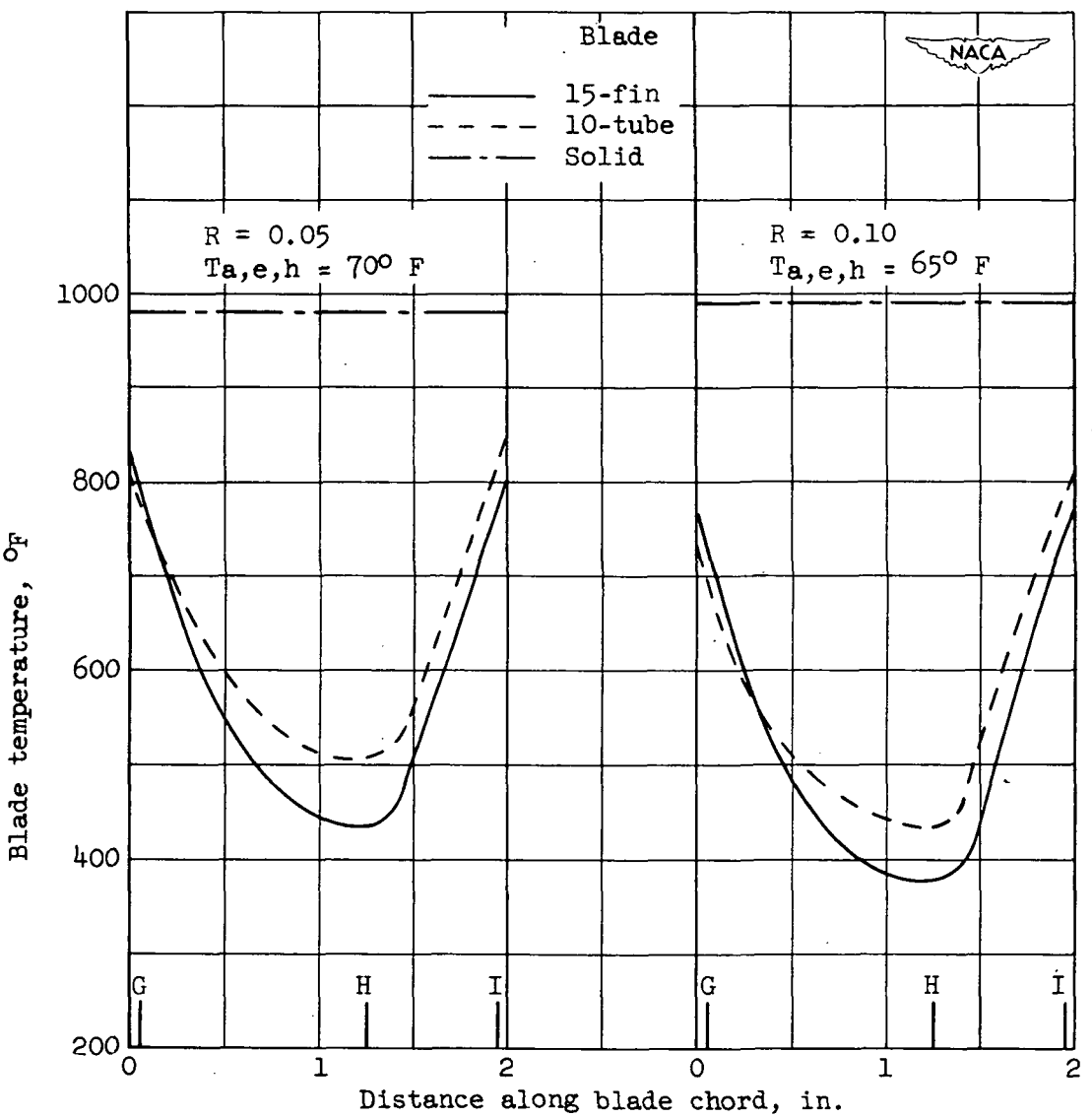

(a) Thermocouples G, H, and I (peripheral, 35-percent span).

Figure 16. - Comparison of blade-temperature distribution along blade chord of 15-fin and 10-tube blades for engine speed of 10,000 rpm.

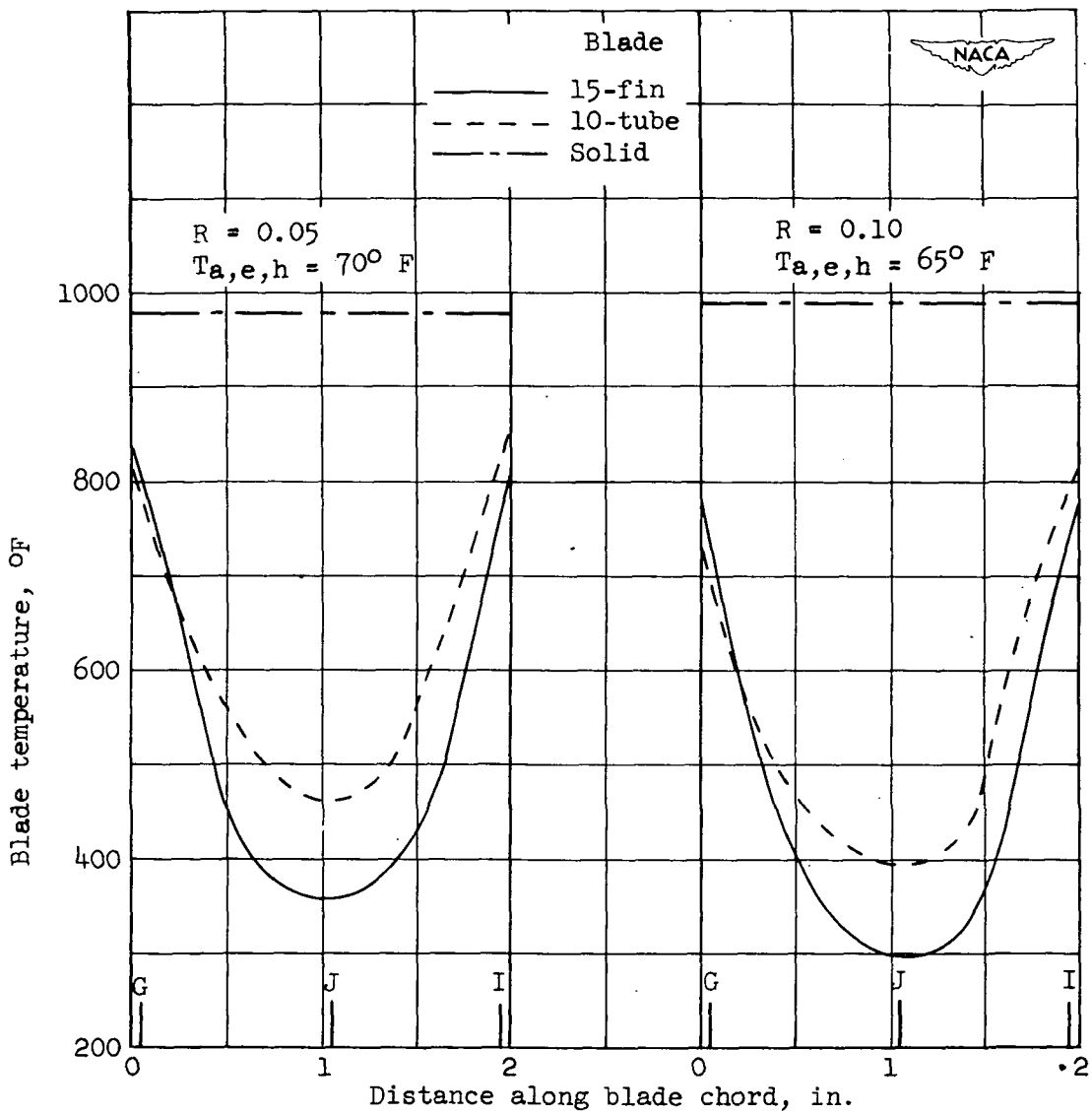

(b) Thermocouples G, J, and I (peripheral, 35-percent span).

Figure 16. - Concluded. Comparison of blade-temperature distribution along blade chord of 15-fin and 10-tube blades for engine speed of 10,000 rpm.

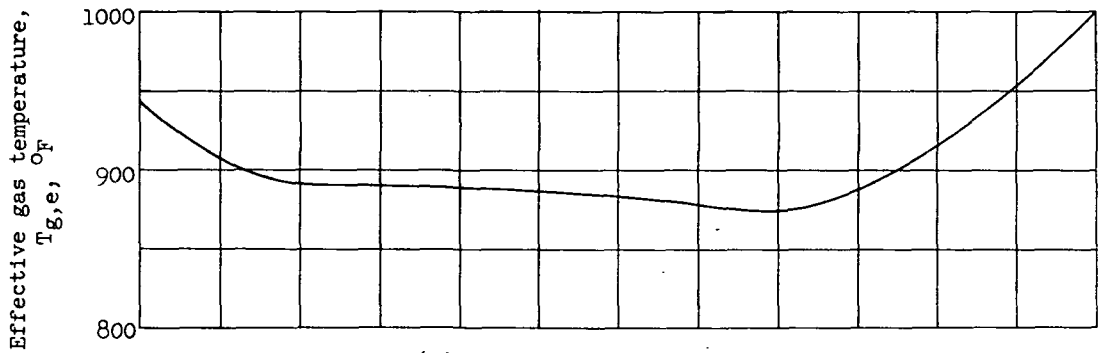

(a) Effective gas temperature.

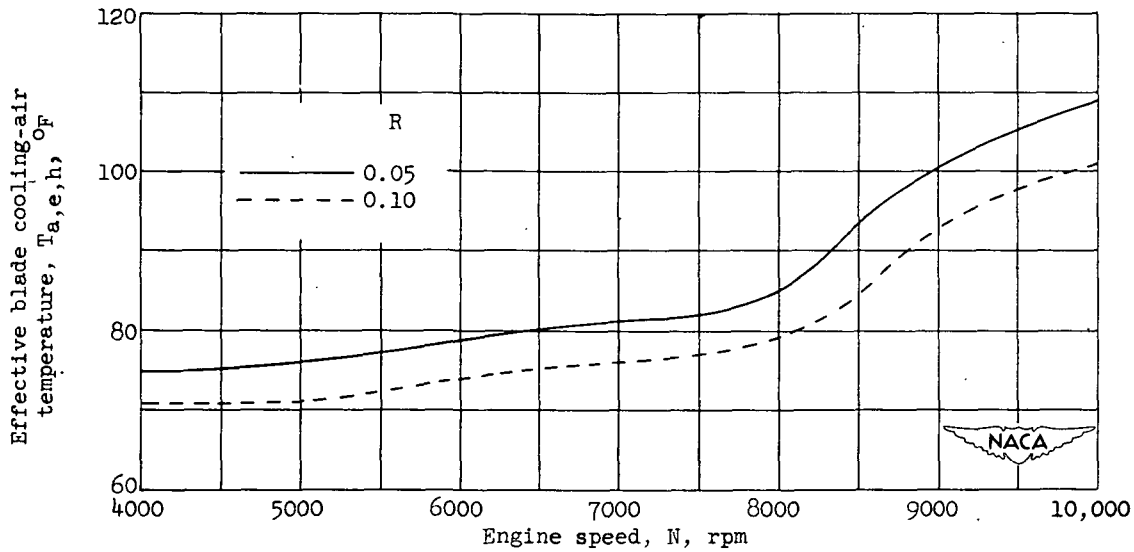

(b) Effective blade cooling-air temperature.

Figure 17. - Variation of effective gas temperature and effective blade cooling-air temperature with engine speed for standard engine-inlet conditions.

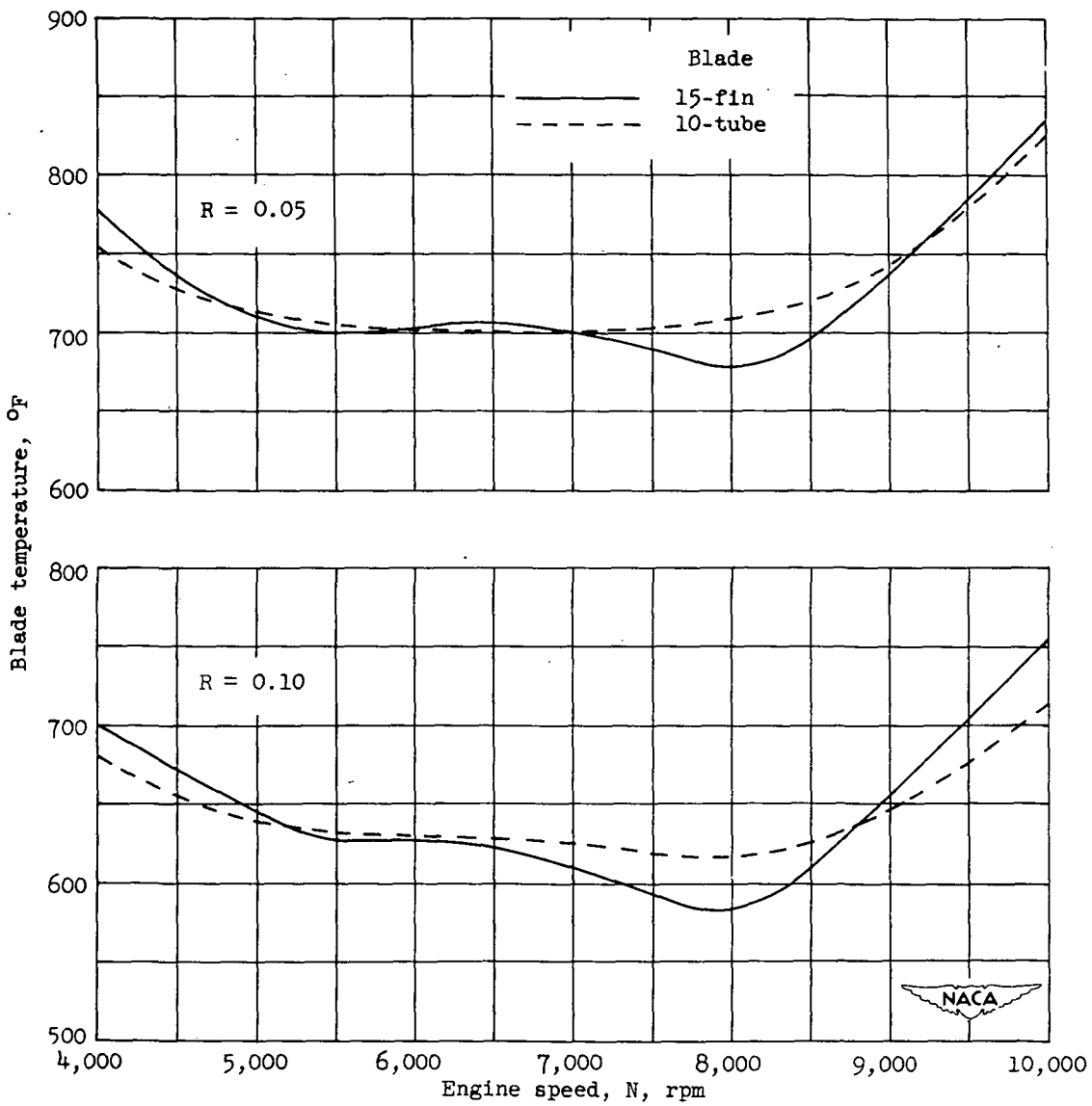

(a) Thermocouple G (leading edge, 35-percent span).

Figure 18. - Comparison of blade temperatures of 15-fin and 10-tube blades over range of engine speeds for standard engine-inlet conditions.

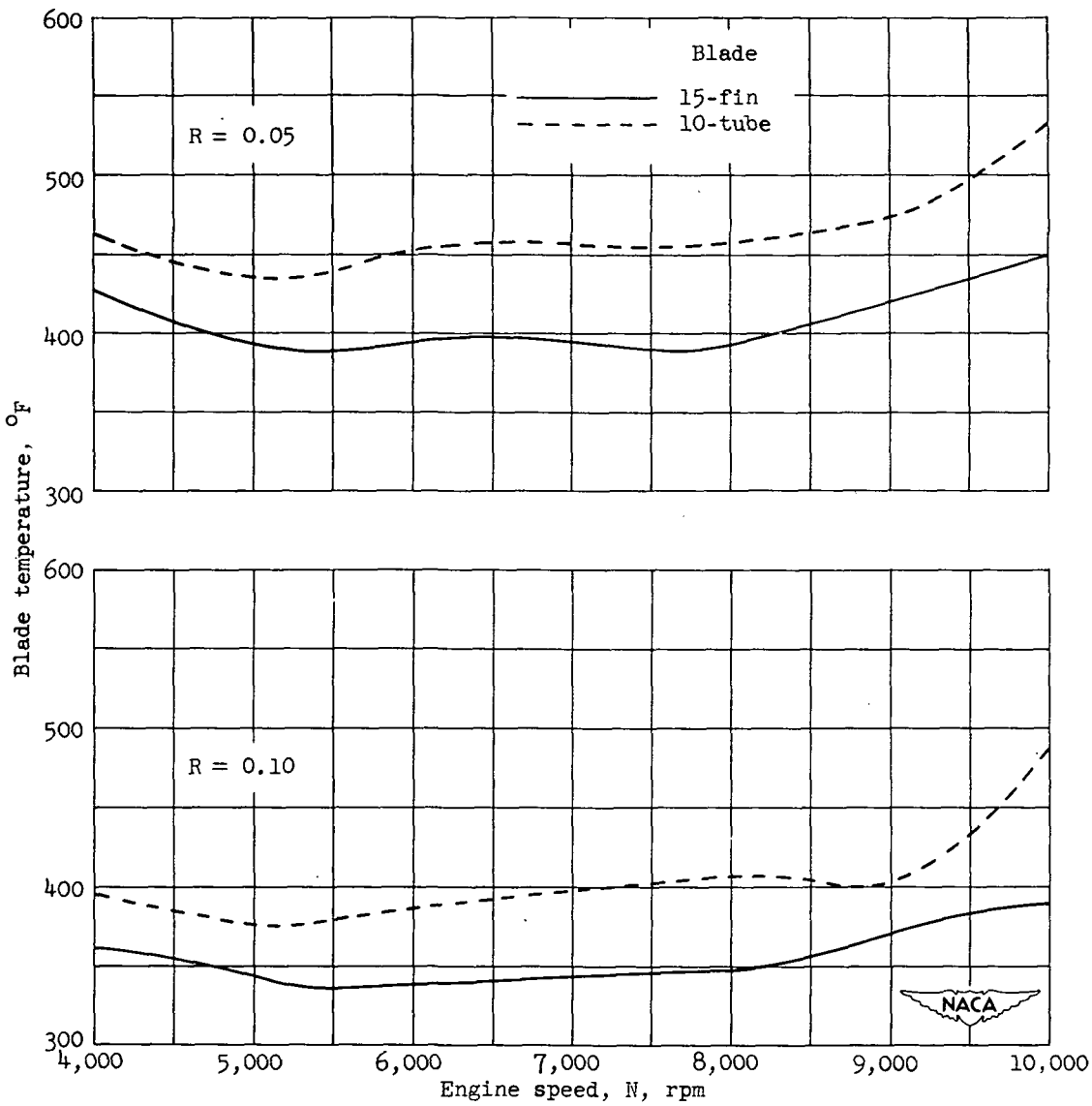

(b) Thermocouple H (midchord, 35-percent span).

Figure 18. - Continued. Comparison of blade temperatures of 15-fin and 10-tube blades over range of engine speeds for standard engine-inlet conditions.

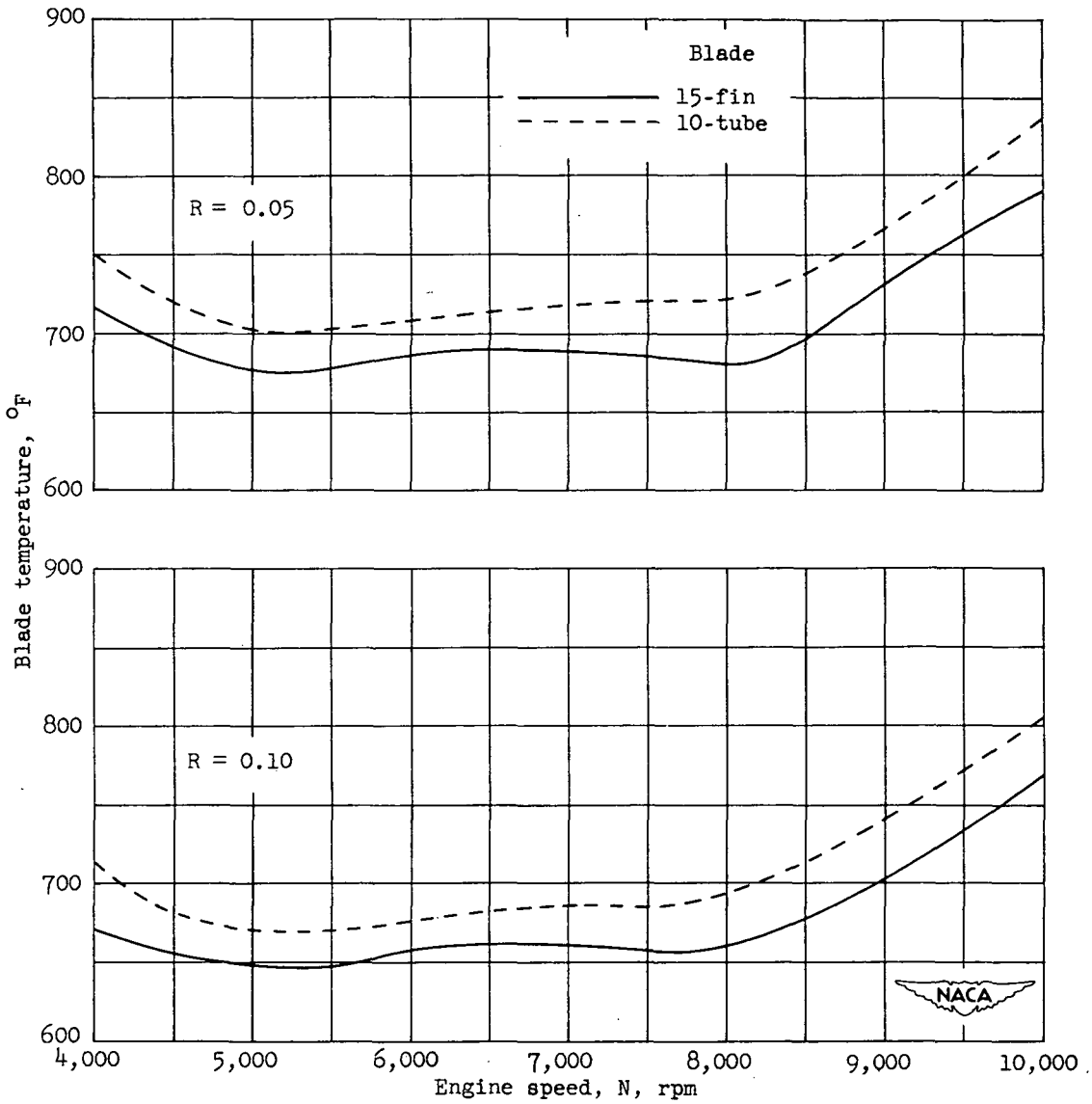

(c) Thermocouple I (trailing edge, 35-percent span).

Figure 18. - Continued. Comparison of blade temperatures of 15-fin and 10-tube blades over range of engine speeds for standard engine-inlet conditions.

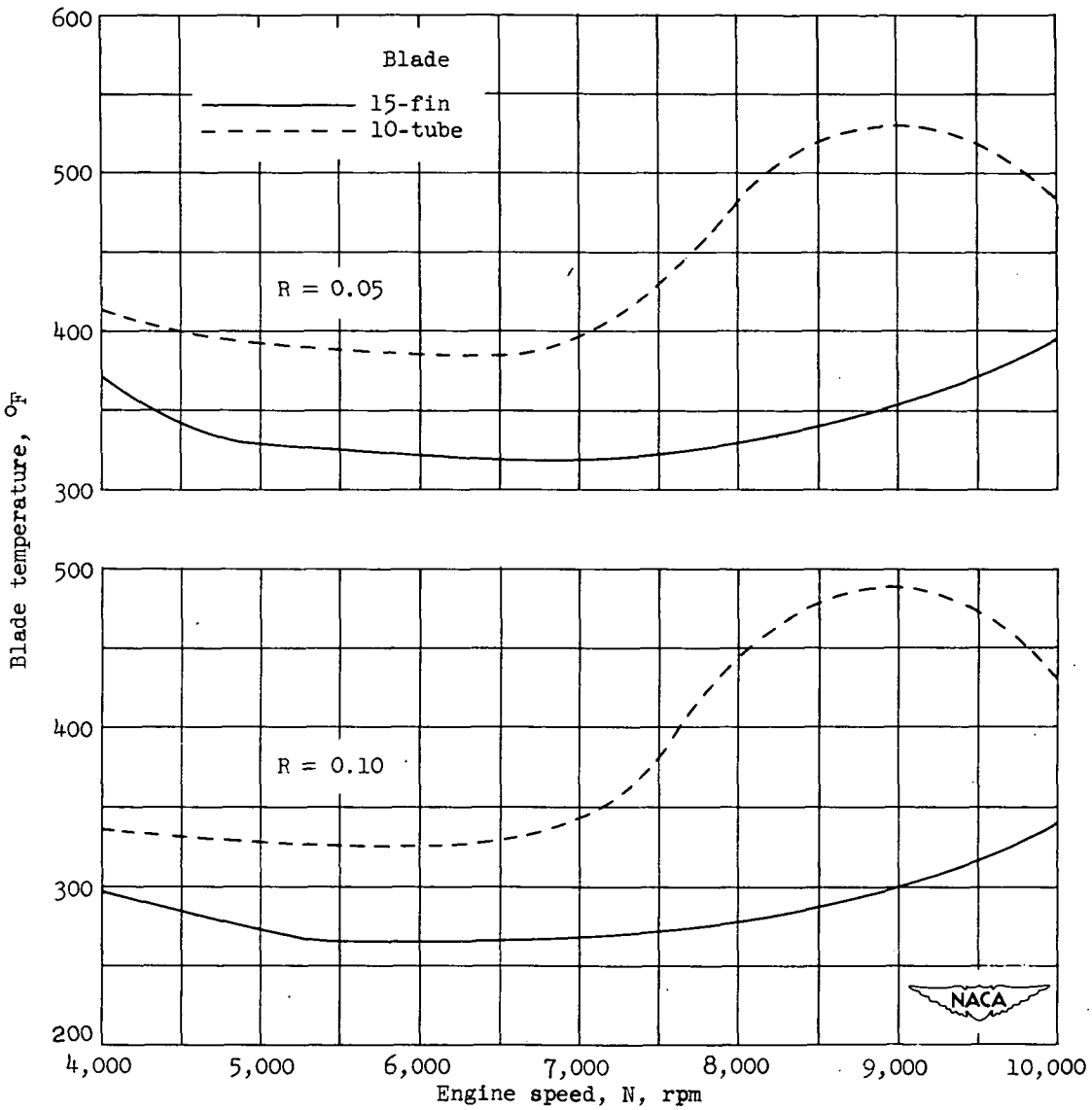

(d) Thermocouple J (midchord, 35-percent span).

Figure 18. - Concluded. Comparison of blade temperatures of 15-fin and 10-tube blades over range of engine speeds for standard engine-inlet conditions.

RETURN TO INSTRUMENT
BRANCH FILE

CLASSIFICATION CHANGED
To Unclassified
By authority of Rocd Record Abstract No 56
12/11/53 Date 1/18/57
mas

RETURN TO INSTRUMENT
BRANCH FILE